

Algorithmic Foundations for the Diffraction Limit

Sitan Chen*
MIT

Ankur Moitra†
MIT

November 28, 2021

Abstract

For more than a century and a half it has been widely-believed (but was never rigorously shown) that the physics of diffraction imposes certain fundamental limits on the resolution of an optical system. However our understanding of what exactly can and cannot be resolved has never risen above heuristic arguments which, even worse, appear contradictory. In this work we remedy this gap by studying the diffraction limit as a statistical inverse problem and, based on connections to provable algorithms for learning mixture models, we rigorously prove upper and lower bounds on how many photons we need (and how precisely we need to record their locations) to resolve closely-spaced point sources.

We give the first provable algorithms that work regardless of the separation, but only for a constant number of point sources. Surprisingly, we show that when the number of point sources becomes large, there is a phase transition where the sample complexity goes from polynomial to exponential, and we pin down its location to within a universal constant that is independent of the number of point sources. Thus it is rigorously possible both to break the diffraction limit and yet to prove strong impossibility results depending on the setup. This is the first non-asymptotic statistical foundation for resolution in a model arising from first principles in physics, and helps clarify many omnipresent debates in the optics literature.

1 Introduction

For more than a century and a half it has been widely-believed (but was never rigorously shown) that the physics of diffraction imposes certain fundamental limits on the resolution of an optical system. In the standard physical setup, we observe incoherent illumination from far-away point sources through a perfectly circular aperture (see Figure 1). Each point source produces a two-dimensional image, originally computed explicitly by Sir George Biddell Airy in 1835 [Air35] and now called an *Airy disk*. The normalized intensity at a point \mathbf{x} on the observation plane is given by

$$I(\mathbf{x}) = \frac{1}{\pi\sigma^2} \left(\frac{2J_1(\|\mathbf{x}\|_2/\sigma)}{\|\mathbf{x}\|_2/\sigma} \right)^2$$

where J_1 is a Bessel function of the first kind. It can be interpreted, e.g. under Feynman’s path integral formalism, as the infinitesimal probability of detecting a photon at some position. The physical properties of the optical system, in particular its numerical aperture and the wavelength of the light being observed, determine σ which governs the amount by which each point source has been blurred.

*This work was supported in part by a Paul and Daisy Soros Fellowship, NSF CAREER Award CCF-1453261, and NSF Large CCF-1565235 and was done in part while S.C. was an intern at Microsoft Research AI.

†This work was supported in part by NSF CAREER Award CCF-1453261, NSF Large CCF-1565235, a David and Lucile Packard Fellowship, and an Alfred P. Sloan Fellowship.

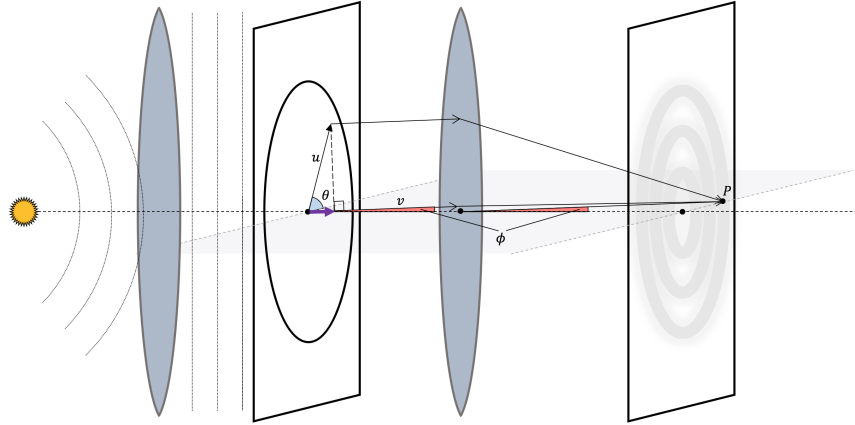


Figure 1: **Fraunhofer diffraction.** Diagram depicts Fraunhofer diffraction of incoherent illumination from point source through a circular aperture onto observation plane

Intuitively, when the point sources are closer together it becomes harder to resolve them. However our understanding of what exactly can and cannot be resolved has been mostly guided by heuristic arguments. In 1879 Lord Rayleigh [Ray79] proposed a criterion for assessing the resolving power of an optical system, which is still widely-used today, of which he wrote:

“This rule is convenient on account of its simplicity and it is sufficiently accurate in view of the necessary uncertainty as to what exactly is meant by resolution.”

Over the years, many researchers have proposed alternative criteria and offered arguments about why some are more appropriate than others. For example, in 1916 Carroll Sparrow proposed a new criterion [Spa16] that bears his name, which he justified as follows:

“It is obvious that the undulation condition should set an upper limit to the resolving power ... The effect is observable both in positives and in negatives, as well as by direct vision ... My own observations on this point have been checked by a number of my friends and colleagues.”

Even more resolution criteria were proposed, both before and after, by Ernst Abbe [Abb73], Sir Arthur Schuster [Sch04], William Houston [Hou27], etc. Their popularity varies depending on the application area and research community. Many researchers have also pushed back on the idea that there is a fundamental diffraction limit at all. In his 1964 Lectures on Physics [FLS11, Section 30-4], Richard Feynman writes:

“... it seems a little pedantic to put such precision into the resolving power formula. This is because Rayleigh’s criterion is a rough idea in the first place. It tells you where it begins to get very hard to tell whether the image was made by one or by two stars. Actually, if sufficiently careful measurements of the exact intensity distribution over the diffracted image spot can be made, the fact that two sources make the spot can be proved even if θ is less than λ/L .”

Or as Toraldo di Francia [DF55] puts it:

“Mathematics cannot set any lower limit for the distance of two resolvable points.”

In this work, we will study the diffraction limit as a statistical inference problem and give the first rigorous and non-asymptotic arguments about what is and is not resolvable.

Question 1.1. *How many samples (i.e. photons) are needed to accurately estimate the centers and relative intensities of a superposition of two or more Airy disks, as a function of their separation and the parameters of the optical system?*

Formally, suppose we are given samples $\mathbf{x}_1, \dots, \mathbf{x}_N$ drawn from a *superposition of k Airy disks*, that is, a distribution with density

$$\rho(\mathbf{x}) = \sum_{i=1}^k \lambda_i \cdot A_\sigma(\|\mathbf{x} - \boldsymbol{\mu}_i\|_2) \quad \text{for} \quad A_\sigma(z) = \frac{1}{\pi\sigma^2} \left(\frac{J_1(z/\sigma)}{z/\sigma} \right)^2,$$

where $\boldsymbol{\mu}_1, \dots, \boldsymbol{\mu}_k$ are the centers of the Airy disks, $\lambda_1, \dots, \lambda_k$ are their relative intensities, and $A_\sigma(z)$ is the (radial) Airy point-spread function (PSF), normalized to be a probability density over \mathbb{R}^2 , where $\sigma \triangleq (\kappa r)^{-1}$ for κ the wavenumber of the light and r the radius of the aperture (see Definition 2.1 for a formal definition, and see Appendix B.2 for a detailed discussion of its physical motivation).

This is essentially equivalent to the *semiclassical detection model* [Goo15], which has received significant attention in the optics literature (see Appendix B.3 for a comparison of the models). It is a natural abstraction that captures experimental limitations like having finite exposure times. Other complexity measures, like the granularity at which we record the locations of the photons, turn out to be equivalent to sample complexity up to polynomial factors. Many researchers have sought to establish fundamental limits to resolution through this model.

Despite the fact that the semiclassical detection model has been studied for decades, existing works fall short of rigorously proving either upper or lower bounds for the problem of learning the centers and relative intensities of a superposition of Airy disks. Some works use more analytically tractable alternatives to the Airy point spread function (e.g. one-dimensional, Taylor approximation, or Gaussian) [Har64, BVDDD⁺99, VAdVDVDB02, Far66, Luc92a]. Others study the problem asymptotically without any finite sample guarantees [Hel64, TD79, RWO06, CWO16, DD96, VDB01]. There is also a substantial body of work studying the simpler *hypothesis testing problem*, in which we are guaranteed that the diffraction pattern comes from either a single Airy disk at the origin, or two equal-intensity Airy disks centered on the x -axis at a *known* distance d apart from each other, and our goal is to determine which case we are in [AH97, Har64, Hel64, Far66]. Most crucially, all works focus solely on superpositions of *two* Airy disks, but as we will see, a sharp statistical theory of the diffraction limit only emerges as the number of Airy disks becomes much larger.

In this sense, our work is conceptually inspired by the literature on provable algorithms for learning mixtures of Gaussians [Das99, MV10, BS15]. Additionally, we note that another line of work [Don92, CFG14] studies the related problem of *superresolution*, i.e. determining locations of spikes from band-limited Fourier measurements, but this model is only an approximation to the physics of diffraction rather than the one that emerges from first principles (see Appendix B for an extensive discussion of the physical motivation for the model we consider).

We provide an overview of the relevant literature from the theoretical computer science and statistics communities in Section 1.2 and from the optics community in Appendix A.

1.1 Overview of Results

In this work we give the first algorithms for learning superpositions of Airy disks with rigorous guarantees on their accuracy, sample complexity, and running time. Along the way, we will answer some of the lingering mysteries surrounding the diffraction limit. Many heuristics [WSS01] for

resolving superpositions of Airy disks seem to succeed well beneath various hypothesized diffraction limits. Do these heuristics actually work or are they merely producing spurious explanations for the diffraction pattern? We show that for any constant number of Airy disks it is possible to resolve them to any desired accuracy regardless of their separation.

Theorem 1.1 (Informal, see Theorem 3.1). *Let ρ be a Δ -separated superposition of k Airy disks where every disk has relative intensity at least λ . Then for any target error $\epsilon > 0$ and failure probability $\delta > 0$, there is an algorithm which draws $N = \text{poly}\left((k\sigma/\Delta)^{k^2}, 1/\lambda, 1/\epsilon, \log(1/\delta)\right)$ samples from ρ , runs in time $O(N)$, and outputs an estimate for the centers and relative intensities of ρ which incurs error ϵ with probability at least $1 - \delta$. Furthermore, this holds even when there is granularity in the photon detector, as long as it is at most some inverse polynomial in N .*

The fact that the diffraction limit can be broken even in the classical physical setup considered here has long been suspected by practitioners and repeatedly claimed in an informal fashion in the statistical optics literature [MW17, BW13, Goo15, DWSD15, DF55, DDVdB97], but proving that you can estimate the true parameters of the model and not just find ones that produce a hypothesis that closely fits the observed diffraction pattern had remained elusive. Without algorithms with provable guarantees, even the most basic methodologies of assessing statistical significance are out of reach. In particular, without lower bounds on the total variation distance between a single Airy disk and a superposition of two Airy disks, it is impossible to compute p -values or control the false discovery rate.

Our algorithm exploits analytic properties of the Airy disk to solve the deconvolution problem, and extends to other well-behaved point spread functions. First we use samples from the model to obtain a point-wise approximation to the Fourier transform $\hat{\rho}$ of the superposition of Airy disks. The Fourier transform $\hat{\rho}$ can be expressed as a product of a complex trigonometric polynomial and the convolution of an indicator function for the ball with itself. By point-wise dividing by an appropriate function inside a ball whose radius corresponds to the Abbe limit, we can simulate noisy access to the Fourier transform of the mixture of point masses located at the centers of ρ . Our access is band-limited so that we can only query at frequencies with bounded L_2 norm. Finally by querying $\hat{\rho}$ at carefully chosen points along a random direction v we can use the matrix pencil method [Moi15] to set up a generalized eigenvalue problem to recover the centers of the Airy disks projected along the direction v . We can then repeat this process for a nearby direction v' and piece together the two one-dimensional estimates to get an accurate two-dimensional estimate for the centers. Once we know the centers, it is straightforward to set up a linear system to solve for the relative intensities. *While this result may be somewhat expected from the perspective of learning mixture models, it demonstrates the insights that these tools can have when brought to bear on new fields like optics.*

From a technical standpoint, the reason for the exponential dependence on k in Theorem 1.1 is that the stability of the matrix pencil method depends on the condition number of a certain Vandermonde matrix. Without additional assumptions on the level of separation between the components, this condition number can very well scale exponentially with k , and in fact this implies an *information-theoretic* lower bound not only for the matrix pencil method, but for any algorithm. In particular, we construct two different superpositions of k tightly spaced Airy disks with very different sets of centers, but where the number of samples needed to distinguish one superposition from the other grows exponentially with k :

Theorem 1.2 (Informal, see Theorem 4.1). *For any $0 < \epsilon < 1$, there exist two superpositions of k Airy disks ρ, ρ' which are both $(1 - \epsilon) \cdot \pi\sigma$ -separated and such that 1) ρ and ρ' have noticeably*

different sets of centers, and yet 2) it would take at least $2^{\Omega(\epsilon k)}$ samples to distinguish whether the samples came from ρ or from ρ' .

Note that the threshold $\pi\sigma$ here corresponds to the so-called *Abbe limit*, and it has been widely accepted in the optics community, albeit without proof, that this threshold marks the theoretical limit for how well point sources of light can be resolved in the classical Fraunhofer diffraction setup.

Näively by parameter counting it ought to be possible to construct two superpositions of k Airy disks whose first $k/2$ moments match exactly. It turns out that this is not quite enough to get bounds on the total variation distance between them that are exponentially small in k . However, by smoothness properties of Airy disks, we can relate the total variation distance to the L_2 -distance. Thus by Plancherel's theorem it suffices to ensure that the Fourier transforms of the superpositions are exponentially close in L_2 -distance. Finally a construction of Moitra [Moi15], building on work of Moitra and Valiant [MV10], can be applied to our setup: by picking the relative intensities of the two superpositions based on convolutions of scalings of the Fejer kernel, we can ensure that the Fourier transforms are sufficiently close in L_2 .

Finally we complete the puzzle (up to a small constant factor) with what we regard as the main technical contribution of this work: We show that when the Airy disks have separation slightly above the diffraction limit, there is an algorithm for resolving them to any desired accuracy whose running time and sample complexity grow only polynomially with k .

Theorem 1.3 (Informal, see Theorem 3.2). *Define the absolute constant $\gamma_{\text{res}} = \frac{2j_{0,1}}{\pi} = 1.530\dots$, where $j_{0,1}$ is the first positive zero of the Bessel function J_0 . Let ρ be a $\gamma_{\text{res}} \cdot \pi\sigma$ -separated superposition of k Airy disks where every disk has relative intensity at least λ . Then for any target error $\epsilon > 0$, there is an algorithm with time and sample complexity $N = \text{poly}(k, 1/\Delta, 1/\lambda, 1/\epsilon)$ which outputs an estimate for the centers and relative intensities of ρ which incurs error ϵ with probability at least $9/10$. Furthermore, this holds even when there is granularity in the photon detector, as long as it is at most some inverse polynomial in all parameters.*

Here we can no longer use the strategy of projecting onto a direction v and applying the matrix pencil method because there are examples of superpositions of Airy disks where the centers are well-separated in two-dimensions but along *any* one-dimensional projection they are not. One way of extending the matrix pencil method to higher dimensions without the need to project is via the tensor decomposition framework of Huang and Kakade [HK15], which they used to get algorithms for the related problem of superresolution in high dimensions where one has access to noisy Fourier measurements, but which are band-limited in L_∞ -distance. Unfortunately, the separation condition they require for the centers is greater than the Abbe limit by a factor scaling *logarithmically in the number of components k* , whereas the heuristic diffraction limits proposed in optics (see Appendix B.4) are all off from the Abbe limit by only *universal constants*.

We argue that this exclusive focus on L_∞ instead of L_2 , not just in [HK15] but in essentially all works on superresolution in high dimensions [CFG14, KPRvdO16, EKPR18, MC16], is one of the main obstacles to getting stronger results that are relevant to optics. First, we sketch the approach of [HK15]. Their idea is to assemble a third-order tensor whose entries consist of noisy Fourier measurements at randomly chosen frequencies. Then by a standard stability analysis of Jennrich's algorithm, Huang and Kakade [HK15] reduce showing correctness of this algorithm to showing the condition number of a certain Vandermonde matrix $V \in \mathbb{C}^{m \times k}$ whose entries depend on the locations of the k centers is polynomially bounded. The off-diagonal entries of $V^\dagger V$ correspond roughly to the level of interaction (in frequency space) between pairs of distinct centers, and they argue that once separation grows logarithmically with k , $V^\dagger V$ becomes diagonally dominant. One could hope for the condition number to be bounded at lower separations where $V^\dagger V$ need not be

diagonally dominant. In the one-dimensional case, Moitra [Moi15] showed this in a strong sense by using the Beurling-Selberg minorant, an extremal function that has found many applications in analytic number theory, as a *universal preconditioner* for $V^\dagger V$, where universal here refers to the fact that the preconditioner does not depend on the specific entries of V .

A natural question to ask is whether higher-dimensional generalizations of the Beurling-Selberg minorant exist, and this is where focusing on L_∞ runs into difficulties: getting the suitable generalization in L_∞ turns out to be a notorious open problem in harmonic analysis, the so-called *box minorant problem* [CGK17]. On the other hand, recall from our sketched proof of Theorem 1.1 that our deconvolution technique can give us L_2 -band-limited access to the Fourier transform. Fortunately, whereas the L_∞ generalization of the Beurling-Selberg minorant is wide open, the L_2 generalization has been completely solved [HV⁺96, CCLM17, Gon18] and was even the workhorse behind recent progress on Montgomery’s famous pair correlation conjecture for the Riemann zeta function [CCLM17]. To the best of our knowledge, this function appears to be new to the theoretical computer science literature. We summarize its properties in Theorem 3.4.

By using the tensor decomposition approach of Huang and Kakade [HK15] and invoking the ball minorant as a universal preconditioner in the analysis, we can circumvent any dependence whatsoever on the number of point sources. In particular, we give the first polynomial-time algorithm that succeeds under a separation condition which is off from the Abbe limit by a (small) universal constant factor. We remark that existing heuristics [WSS01] in the optics literature rely on brute-force search and run in time exponential in k .

The main open question in our work is to close the constant factor gap between Theorem 1.2 and Theorem 1.3, which seems to require new tools from harmonic analysis.

1.2 Related Work

While our work is thematically most closely related to the broader agenda of applying theoretical computer science as a lens on the natural sciences, there are two areas of theoretical machine learning and statistics from which this paper draws conceptual and technical inspiration: learning mixture models and resolving spike trains from low frequency measurements – i.e. super-resolution. We now elaborate on how our contributions fit into these lines of work.

Mixture Models The question of learning the parameters of mixtures of structured distributions has a vast literature that we cannot hope to fully survey here. As mentioned previously, this paper was conceptually inspired in part by the line of work on developing provable algorithms for learning mixtures of Gaussians [Das99, DS00, AK01, VW02, AM05, BV08, KMV10, MV10, BS15, HP15, HK13, GHK15, RV17, HL18, KS17, DKS18]. In one sense, the difference between our model and the one considered there is merely a different choice of kernel. In particular, rather than observing data which is generated by convolving a mixture of point sources with a Gaussian, we convolve with an *Airy disk* instead. Let us call it A_σ . This change is important because our generative model is one that actually comes from first principles in physics and is an extremely accurate approximation in some settings like astronomy (see Appendix A for a detailed discussion about the physical motivation of the model). From a technical standpoint, this new choice of kernel also introduces a number of analytic complications. In addition to the highly oscillatory nature of the Bessel function J_1 in the definition of A_σ , A_σ does not even possess a finite second moment, precluding a straightforward adaptation of most of the existing techniques for learning mixture models which revolve around method of moments. We do, however, make key use of the idea of learning the mixture by learning its parameters along one dimensional projections, a technique notably employed by [KMV10, MV10] for learning mixtures of Gaussians.

That said, arguably the part of this literature that is most relevant to our work is the information-theoretic *lower bounds* for learning mixtures of Gaussians, first shown by [MV10] and subsequently refined by [HP15, RV17]. One trick from these works is to upper bound the total variation distance between two mixtures by invoking Plancherel’s and smoothness properties of the kernel, in their case the Gaussian, to reduce to upper bounding the L_2 distance of the *Fourier transforms* of the mixtures. We essentially follow this outline, though our analysis for upper bounding the distance between the Fourier transforms is quite different from the corresponding analysis in these works.

Lastly, we compare the phase transition we show here versus what is known for clustering spherical mixtures of Gaussians. Regev and Vijayaraghavan [RV17] show that at separation $\Omega(\sqrt{\log k})$, learning is possible with a polynomial number samples, while at separation $o(\sqrt{\log k})$ it requires a superpolynomial number of samples. Note that the phase transition we show is more dramatic: there exist *universal constants* $C \approx 1.530$ and $c = 1$ and a hard threshold, the Abbe limit $\tau \triangleq \pi \cdot \sigma$, such that at any separation strictly greater than $C\tau$, learning a superposition of Airy disks only requires $\text{poly}(k)$ samples, and at any separation strictly less than $c\tau$, it requires sample complexity exponential in k .

Superresolution The algorithmic results of this work draw some inspiration from the separate, rich line of work in the statistics literature on superresolution, i.e. estimating spike trains from band-limited, noisy Fourier measurements. The seminal work of [DS89, Don92] was one of the first to put this question on rigorous footing. Donoho studied the modulus of continuity for this problem on a grid as the grid width goes to zero. Later Candes and Fernandez-Granda [CFG14] gave a practical algorithm based on L_1 minimization over a continuous domain. There has been a long line of work on this problem which it would also be impossible to survey fully, so we refer the reader to [CFG13, TBSR13, FG13, Lia15, Moi15, FG16, KPRvdO16, MC16] and references therein. While these works share some motivations with ours, an important distinction is that our model comes from first principles in physics and arises naturally from the path integral formalism for Fraunhofer diffraction and the corresponding mechanism by which photon detectors operate.

The two works in this literature which are most related to ours are that of Moitra [Moi15] analyzing the matrix pencil method and establishing a sharp phase transition at the diffraction limit for *one-dimensional superresolution*, as well as the work of Huang and Kakade [HK15] giving a tensor decomposition algorithm for superresolution in high dimensions given noisy measurements at *random frequencies* rather than at frequencies on some prescribed grid. Our algorithm for Theorem 1.1 also uses the matrix pencil method, though there are key challenges in working in two dimensions rather than one. Huang and Kakade [HK15] tackle this more challenging setting, and we draw upon their tensor decomposition approach in our proof of Theorem 3.2, but as described in Section 1.1, their techniques necessarily fall short of working when the separation condition is not allowed to grow with the number of point sources. This is particularly problematic for the setting of optical resolution, as the various alternative diffraction limits formulated by physicists (see Appendix B.4 for a comprehensive survey of these limits) – that have been used to guide our practical understanding of when resolution is possible – operate within a universal constant factor of the Abbe limit. Additionally, as discussed previously, essentially all works on superresolution in high dimensions focus on the case where measurements are L_∞ band-limited rather than L_2 -band-limited. Given the prevalence of Airy disks and circular apertures in statistical optics, one upshot of our work is that, technical issues related to the box minorant problem notwithstanding, the L_2 setting may be the more practically relevant one to consider anyways.

Further Connections There are also connections to the extensive literature on the sparse Fourier transform, which can be interpreted in some sense as the “agnostic” version of the superresolution

problem where the goal is to compete with the error of the best k -sparse approximation to the discrete Fourier transform, even in the presence of noise, using few measurements [GGI⁺02, GMS05, HIKP12, GIIS14, IKP14, Kap16]. When the k spikes need not be at discrete locations and the low-frequency measurements are randomly chosen, this is the problem of *compressed sensing off the grid* introduced by [TBSR13], for which recovery is possible with far fewer measurements. This can be thought of as the one-dimensional case of the setting of [HK15].

1.3 Visualizing the Diffraction Limit

In this short section we provide some figures to help conceptualize our results. Figure 2 illustrates the basic notion that separation is information-theoretically unnecessary for parameter learning of superpositions of Airy disks. We compare the discretized empirical distribution of samples from two diffraction patterns whose components have separation well below the diffraction limit and thus well below what conventional wisdom in optics suggests is resolvable. While the differences in the diffraction patterns are minute, they do indeed become statistically significant with enough samples. Eventually it becomes possible to conclude that the gray diffraction pattern is generated by one point source and the red diffraction pattern is generated by two.

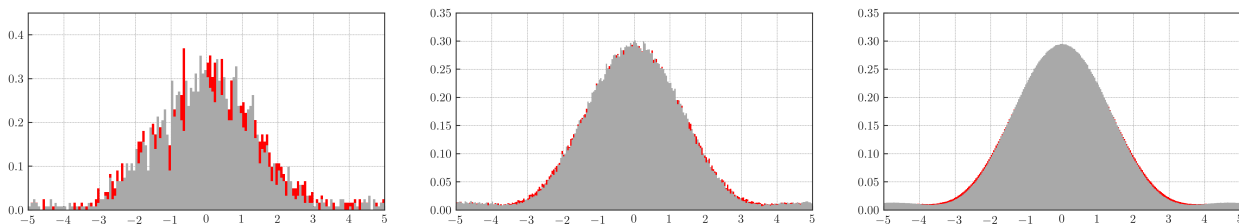


Figure 2: **With enough samples, one can distinguish which of two superpositions the data comes from, even below the diffraction limit.** In each plot, a histogram of x -axis positions of photons sampled from a superposition of two equal-intensity Airy disks (red) centered on the x -axis with separation a tenth of the Abbe limit is overlaid with a histogram of x -axis positions of photons sampled from a single Airy disk at the origin (gray). As number of samples increases (left to right), minute differences between the two intensity profiles become clear.

Next, we present a striking visual representation of the statistical barrier imposed by the diffraction limit when the number of components is large. Recall that the upshot of Theorems 1.2 and 1.3 is that k plays a leading role in determining when resolution is and is not feasible: slightly above the Abbe limit, the sample (and computational) complexity is polynomial in k , and anywhere beneath the Abbe limit, the sample complexity becomes exponential in k . This helps clarify why in some domains like astronomy, where there are only ever a few tightly spaced point sources, there is evidently no diffraction limit. Yet in other domains like microscopy where there are a large number of tightly spaced objects, the diffraction limit is indeed a fundamental barrier, at least in the classical physical setup. This helps explain why different communities have settled on different beliefs about whether there is or is not a diffraction limit.

In Figure 3 we experimentally investigate this phenomenon and illustrate how the total variation distance scales as we vary the number of disks and the separation in our earlier constructions. It is evident from these plots that for any superposition of a few Airy disks, there is no sharp dividing line between what is and is not possible to resolve. But when the number of Airy disks becomes large, with any reasonable number of samples, it is feasible to resolve the superposition if and only if their separation is at least as large as the Abbe limit.

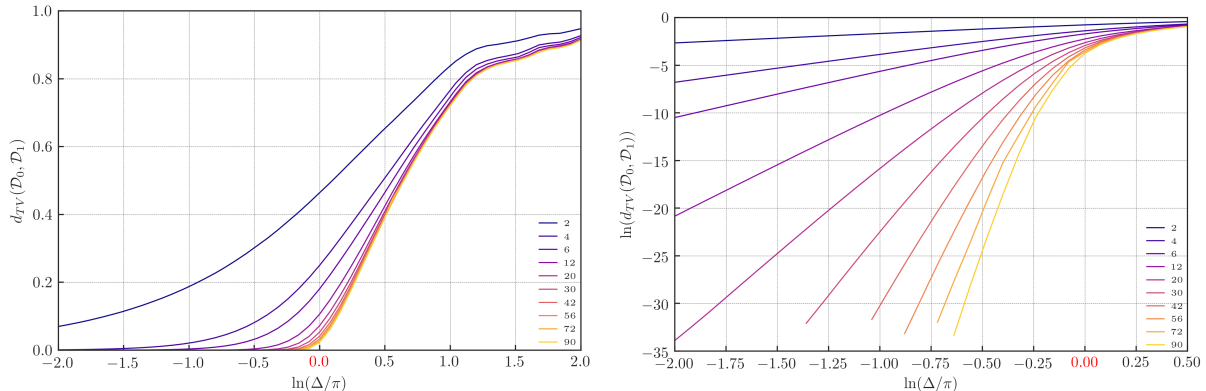


Figure 3: **The Abbe limit as a statistical phase transition.** For any level of separation Δ and number of disks k , we carefully construct a pair of hypotheses $\mathcal{D}_0(\Delta, k), \mathcal{D}_1(\Delta, k)$ which are each superpositions of $k/2$ Airy disks where the separation among its components is at least Δ . The left figure plots total variation distance $d_{TV}(\mathcal{D}_0(\Delta, k), \mathcal{D}_1(\Delta, k))$ between the two distributions as a function of Δ , for various choices of k , with the Abbe limit highlighted in red. The right figure plots total variation distance on a log-scale.

We emphasize that in the instance constructed for Figure 3 (as well as the instance we construct and analyze for Theorem 1.2), the centers are plotted on a line. For such instances, by projecting in the direction of the line and using our deconvolution techniques, one can actually reduce to the problem of one-dimensional superresolution, for which polynomial-time algorithms exist for *any* separation strictly greater than the diffraction limit [Moi15], matching our lower bound. In contrast, if the centers can be placed anywhere in \mathbb{R}^2 , there is a constant factor gap between our lower bound and our Theorem 1.3.

1.4 Roadmap

In Section 2 we give an overview of our probabilistic model, some notation, and other mathematical preliminaries. In Section 3, we prove the algorithmic results sketched in Theorems 1.1 and 1.3. In Section 4 we prove the information-theoretic lower bound sketched in Theorem 1.2. In Appendix A, we overview previous attempts in the optics literature to put the diffraction limit on rigorous footing. In Appendix B, we describe and motivate our model and also define the various resolution criteria which have appeared in the literature. In Appendix C, we catalogue quotations from the literature that are representative of the points of view addressed in the introduction. In Appendix D, we complete some deferred proofs. Lastly, in Appendix E, we give details on how Figure 3 was generated.

2 Preliminaries

In this section we explain the terminology and notation that we will adopt in this work and also provide some technical preliminaries that will be useful later.

Generative Model We first formally define the family of distributions we study in this work.

Definition 2.1. [Superpositions of Airy Disks] A superposition of k Airy disks ρ is a distribution over \mathbb{R}^2 specified by relative intensities $\lambda_1, \dots, \lambda_k \geq 0$ summing to 1, centers $\mu_1, \dots, \mu_k \in \mathbb{R}^2$, and an

a priori known “spread parameter” $\sigma > 0$. Its density is given by

$$\rho(\mathbf{x}) = \sum_{i=1}^k \lambda_i \cdot A_\sigma(\mathbf{x} - \boldsymbol{\mu}_i) \quad \text{for} \quad A_\sigma(\mathbf{z}) = \frac{1}{\pi\sigma^2} \left(\frac{J_1(\|\mathbf{z}\|_2/\sigma)}{\|\mathbf{z}\|_2/\sigma} \right)^2.$$

Note that the factor of $\frac{1}{\pi\sigma^2}$ in the definition of A_σ is to ensure that $A_\sigma(\cdot)$ is a probability density.

Also define

$$\Delta \triangleq \min_{i \neq j} \|\boldsymbol{\mu}_i - \boldsymbol{\mu}_j\|_2 \quad \text{and} \quad \mathcal{R} \triangleq \max_{i \in [k]} \|\boldsymbol{\mu}_i\|_2.$$

It will be straightforward to extend the above model to take into account error stemming from the fact that the photon detector itself only has finite precision.

Definition 2.2 (Discretization Error). *Given discretization parameter $\varsigma > 0$, we say \mathbf{x} is a ς -granular sample from ρ if it is produced via the following generative process: 1) a point \mathbf{x}' is sampled from ρ , 2) \mathbf{x} is obtained by moving \mathbf{x}' an arbitrary distance of at most ς .*

Fourier Transform We will use the following convention in defining the Fourier transform. Given $f \in L_2(\mathbb{R}^d)$,

$$\hat{f}(\boldsymbol{\omega}) \triangleq \int_{\mathbb{R}^d} f(\mathbf{x}) \cdot e^{-2\pi i \langle \boldsymbol{\omega}, \mathbf{x} \rangle} d\mathbf{x}. \quad (1)$$

Optical Transfer Function The following is a standard calculation.

Fact 1. $\hat{A}_\sigma[\boldsymbol{\omega}] = \frac{2}{\pi} (\arccos(\pi\sigma\|\boldsymbol{\omega}\|) - \pi\sigma\|\boldsymbol{\omega}\| \sqrt{1 - \pi^2\sigma^2\|\boldsymbol{\omega}\|^2}).$

Proof. It is enough to show this for $\sigma = 1$. Let $G(\mathbf{x}) \triangleq J_1(\|\mathbf{x}\|)/\|\mathbf{x}\|$. It is a standard fact that the zeroth-order Hankel transform of the function $r \mapsto J_1(r)/r$ is the indicator function of the interval $[0, 1]$. Using our convention for the Fourier transform (see (1)), this implies that $\hat{G}[\boldsymbol{\omega}] = 2\pi \cdot \mathbb{1}[\|\boldsymbol{\omega}\| \in [0, 1/2\pi]]$. Because $A_1 = G^2/\pi$, by the convolution theorem we conclude that \hat{A}_1 is $\frac{1}{\pi}$ times the convolution of \hat{G} with itself, which is just $4\pi^2$ times the convolution of the indicator function of the unit disk of radius $1/2\pi$ with itself. By elementary Euclidean geometry one can compute this latter function to be $\boldsymbol{\omega} \mapsto \frac{1}{2\pi^2} \cdot \left(\arccos(\pi\|\boldsymbol{\omega}\|) - \pi\|\boldsymbol{\omega}\| \sqrt{1 - \pi^2\|\boldsymbol{\omega}\|^2} \right)$, from which the claim follows. \square

In optics, the two-dimensional Fourier transform of the point-spread function is called the *optical transfer function*, a term we will occasionally use in the sequel.

Now note that by Fact 1, \hat{A}_σ is supported only over the disk of radius $\frac{1}{\pi\sigma}$ centered at the origin in the frequency domain. In the spatial domain, this corresponds to a separation of $\pi\sigma$; this is the definition of the *Abbe limit*. We will need the following elementary estimate for $\hat{A}[\boldsymbol{\omega}]$:

Fact 2. *For all $\|\boldsymbol{\omega}\|_2 \leq 1$, $\hat{A}[\boldsymbol{\omega}] \geq (1 - \|\boldsymbol{\omega}\|_2)^2$.*

Scaling As the algorithms we give will be scale-invariant, we will assume that $\sigma = 1/\pi$ in the rest of this work and refer to $A_{1/\pi}$ as A .

Parameter Estimation Accuracy The following terminology formalizes what it means for an algorithm to return an accurate estimate for the parameters of a superposition of Airy disks.

Definition 2.3. $(\{\lambda_i^*\}_{i \in [k]}, \{\mu_i^*\}_{i \in [k]})$ is an (ϵ_1, ϵ_2) -accurate estimate for the parameters of a superposition of k Airy disks ρ with centers $\{\mu_i\}$ and relative intensities $\{\lambda_i\}$ if there exists a permutation τ for which

$$\|\mu_i - \tilde{\mu}_{\tau(i)}\|_2 \leq \epsilon_1 \quad \text{and} \quad |\lambda_i - \tilde{\lambda}_{\tau(i)}| \leq \epsilon_2$$

for all $i \in [k]$.

Generalized Eigenvalue Problems Given matrices M, N , we will denote by (M, N) the *generalized eigenvalue problem* $Mx = \lambda Nx$. In any solution (λ, x) to this, λ is called a *generalized eigenvalue* and x is called a *generalized eigenvector*.

Bessel Function Estimates In Section 4, we need the following estimate for $J_\nu(z)$:

Theorem 2.1 ([Lan00]). For some absolute constant $c_1 = 0.7857\dots$, we have for all $\nu \geq 0$ and $r \in \mathbb{R}$ that $|J_\nu(r)| \leq c_1 |r|^{-1/3}$.

Matrices, Tensors, and Flattenings Given a matrix $M \in \mathbb{C}^{a \times b}$, we will denote its i -th row vector by M_i , its j -th column vector by M^j , and its (i, j) -th entry by $M_{i,j}$.

Given a tensor $\mathbf{T} \in \mathbb{C}^{m_1 \times m_2 \times m_3}$ and matrices $M_1 \in \mathbb{C}^{m_1 \times m'_1}$, $M_2 \in \mathbb{C}^{m_2 \times m'_2}$, and $M_3 \in \mathbb{C}^{m_3 \times m'_3}$, define the flattening $\mathbf{T}(M_1, M_2, M_3) \in \mathbb{C}^{m'_1 \times m'_2 \times m'_3}$ by

$$\mathbf{T}(M_1, M_2, M_3)_{i_1, i_2, i_3} = \sum_{(j_1, j_2, j_3) \in [m_1] \times [m_2] \times [m_3]} \mathbf{T}_{m_1, m_2, m_3} \cdot (M_1)_{j_1, i_1} (M_2)_{j_2, i_2} (M_3)_{j_3, i_3}$$

for all $(i_1, i_2, i_3) \in [m'_1] \times [m'_2] \times [m'_3]$.

Miscellaneous Notation Let \mathbb{S}^{d-1} denote the Euclidean unit sphere. Given $r > 0$, let $B^d(r)$ denote the Euclidean ball of radius r centered at the origin in \mathbb{R}^d .

3 Learning Superpositions of Airy Disks

In this section we present the technical details of our algorithmic results. In Sections 3.2 and 3.4, we prove the following formal version of Theorem 1.1.

Theorem 3.1. Let ρ be a Δ -separated superposition of k Airy disks with minimum mixing weight λ_{\min} and such that $\|\mu_i\| \leq \mathcal{R}$ for all $i \in [k]$.

For any $\epsilon_1, \epsilon_2 > 0$, there is some $\alpha = \text{poly}\left(\log 1/\delta, 1/\lambda_{\min}, 1/\epsilon_1, 1/\epsilon_2, \mathcal{R}, (k\sigma/\Delta)^{k^2}\right)^{-1}$ for which there exists an algorithm with time and sample complexity $\text{poly}(1/\alpha)$ which, given $\varsigma = \text{poly}(\alpha)$ -granular sample access to ρ , outputs an (ϵ_1, ϵ_2) -accurate estimate for the parameters of ρ with probability at least $1 - \delta$.

Specifically, in Section 3.2, we show how one can use the matrix pencil method to recover the parameters for ρ given oracle access to the *optical transfer function*, i.e. the two-dimensional Fourier transform of ρ , up to some small additive error. In Section 3.4, we show how to implement this approximate oracle.

In Section 3.3, we also use the oracle of Section 3.4 to prove the following formal version of Theorem 1.3.

Theorem 3.2. Let ρ be a Δ -separated superposition of k Airy disks with minimum mixing weight λ_{\min} and such that $\|\mu_i\| \leq \mathcal{R}$ for all $i \in [k]$. Let

$$\gamma_{\text{res}} = \frac{2j_{0,1}}{\pi} = 1.530\dots, \quad (2)$$

where $j_{0,1}$ is the first positive zero of the Bessel function of the first kind J_0 . For any $\Delta > \gamma_{\text{res}} \cdot \pi \cdot \sigma$, the following holds:

For any $\epsilon_1, \epsilon_2 > 0$, there is some $\alpha = 1/\text{poly}(k, \mathcal{R}, \sigma/\Delta, 1/\lambda_{\min}, 1/\epsilon_1, 1/\epsilon_2, 1/(\Delta - \gamma_{\text{res}}))$ for which there exists an algorithm with time and sample complexity $\text{poly}(1/\alpha)$ which, given $\text{poly}(\alpha)$ -granular sample access to ρ , outputs an (ϵ_1, ϵ_2) -accurate estimate for the parameters of ρ with probability at least $4/5$.

3.1 Reduction to 2D Superresolution

In this section we reduce the problem of learning superpositions of Airy disks to the problem of learning a convex combination of Dirac deltas given the ability to make noisy, band-limited Fourier measurements.

Formally, suppose we had access to the following oracle:

Definition 3.1. An m -query, η -approximate OTF oracle \mathcal{O} takes as input a frequency $\omega \in \mathbb{R}^2$ and, given frequencies $\omega_1, \dots, \omega_m$, outputs numbers $u_1, \dots, u_m \in \mathbb{R}$ for which $|u_j - \widehat{\rho}[\omega_j]| \leq \eta$ for all $j \in [m]$.

Remark 3.1. As we will see in Section 3.4, \mathcal{O} will be constructed by sampling some number of points from ρ and computing empirical averages. The number m and accuracy η of queries that \mathcal{O} can answer dictates the sample complexity of this procedure. As we will see in the proofs of Lemma 3.6 and Lemma 3.12 below, the m that we need to take will be small, so the reader can ignore m and pretend it is unbounded for most of this section.

Given $\omega \in \mathbb{R}^2$, the Fourier transform of ρ evaluated at frequency ω is given by

$$\widehat{\rho}[\omega] = \sum_{j=1}^k \lambda_j \widehat{A}[\omega] e^{-2\pi i \langle \mu_j, \omega \rangle}, \quad (3)$$

where for $\omega = (r \cos \theta, r \sin \theta)$, we have by Fact 1 that

$$\widehat{A}[\omega] = \frac{2}{\pi} (\arccos(r) - r \sqrt{1 - r^2}).$$

In particular, $\widehat{A}[\omega]$ only depends on $r = \|\omega\|$ (because $A(\cdot)$ is radially symmetric), so henceforth regard \widehat{A} as a function merely of r .

Define

$$F(\omega) = \sum_{j=1}^k \lambda_j e^{-2\pi i \langle \mu_j, \omega \rangle}.$$

This is a trigonometric polynomial to which we have noisy pointwise access using \mathcal{O} :

Lemma 3.1. Let $0 < r < 1$. With an η -approximate OTF oracle \mathcal{O} , on input $\omega \in B^2(r)$ we can produce an estimate of $F(\omega)$ to within $\eta/\widehat{A}[r]$ additive error.

Proof. By dividing by $\widehat{A}[\omega]$ on both sides of (3), we get that

$$\frac{\widehat{\rho}[\omega]}{\widehat{A}[\|\omega\|]} = \sum_{j=1}^k \lambda_j e^{-2\pi i \langle \boldsymbol{\mu}_j, \omega \rangle},$$

so given that \mathcal{O} , on input ω , outputs $u \in \mathbb{R}$ satisfying $|u - \widehat{\rho}[\omega]| \leq \eta$, we have that

$$\left| \frac{u}{\widehat{A}[\|\omega\|]} - F(\omega) \right| \leq \frac{\eta}{\min_{0 \leq r' \leq r} \widehat{A}[r']} = \frac{\eta}{\widehat{A}[r]},$$

where the last step uses the fact that $\widehat{A}[\cdot]$ is decreasing on the interval $[0, 1]$. \square

So concretely, given an η -approximate OTF oracle, we have reduced the problem of learning superpositions of Airy disks to that of recovering the locations of $\{\boldsymbol{\mu}_j\}$ given the ability to query $F(\omega)$ at arbitrary frequencies ω for which $\|\omega\|_2 < 1$ to within additive accuracy $\eta/\widehat{A}[\|\omega\|_2]$.

Lastly, for reasons that will become clear in subsequent sections (see e.g. (13)), it will be convenient to assume that $\mathcal{R} \leq 1/3$. This is without loss of generality, as otherwise, we can scale the data down by a factor of $3\mathcal{R}$ so that they are now i.i.d. samples from the superposition of Airy disks with density $\rho'(\mathbf{x}) \triangleq \sum_{j=1}^k \lambda_j \cdot A_{1/\mathcal{R}}(\mathbf{x} - \boldsymbol{\mu}_j/\mathcal{R})$. Define the rescaled centers $\boldsymbol{\mu}'_j \triangleq \boldsymbol{\mu}_j/\mathcal{R}$ and note that by assumption, $\|\boldsymbol{\mu}'_j\|_2 \leq 1/3$ for all $j \in [k]$.

The Fourier transform of ρ' is then given by $\widehat{\rho}'(\omega) = \widehat{A}_{1/\mathcal{R}}[\omega] \sum_{j=1}^k \lambda_j e^{-2\pi i \langle \boldsymbol{\mu}'_j, \omega \rangle}$, so by the proof of Lemma 3.1 we conclude that with an η -approximate OTF oracle for ρ , for any $0 < r < 1$ on input $\omega \in B^2(r \cdot \mathcal{R})$ we can produce an estimate of $\sum_{j=1}^k \lambda_j e^{-2\pi i \langle \boldsymbol{\mu}'_j, \omega \rangle}$ to within $\eta/\widehat{A}[r]$ additive error. Recovering the centers $\{\boldsymbol{\mu}'_j\}$ to within additive error ϵ then translates to recovering the centers $\{\boldsymbol{\mu}_j\}$ to within additive error $3\mathcal{R}\epsilon$. For this reason, we will henceforth assume that $\mathcal{R} \leq 1/3$.

3.2 Learning via the Optical Transfer Function

Our basic approach is as follows. To solve the superresolution problem of Section 3.1, we will project in two random, correlated directions $\omega_1, \omega_2 \in \mathbb{R}^2$ and solve the resulting one-dimensional superresolution problems via matrix pencil method (see MODIFIEDMPM) to recover the projections of $\boldsymbol{\mu}_1, \dots, \boldsymbol{\mu}_k$ in the directions ω_1 and ω_2 , as well as the relative intensities $\lambda_1, \dots, \lambda_k$. From these projections we can then recover the actual centers for ρ by solving a linear system (PRECONSOLIDATE). Such an approach already achieves constant success probability, and we can amplify this by repeating and running a simple clustering algorithm (see SELECT). The full specification of the algorithm is given as LEARNAIRYDISKS.

3.2.1 Learning in a Random Direction

Fix a unit vector $v \in \mathbb{S}^1$. We first show how to leverage Lemma 3.1 and the matrix pencil method to approximate the projection of $\boldsymbol{\mu}_1, \dots, \boldsymbol{\mu}_k$ along v .

By the discussion at the end of Section 3.1, we may assume $\|\boldsymbol{\mu}_i\|_2 \leq 1/2$ for all $i \in [k]$, so $\|\boldsymbol{\mu}_i - \boldsymbol{\mu}_j\|_2 \leq 1$ for all $i \neq j$. For $j \in [k]$, let $m_j = \langle \boldsymbol{\mu}_j, v \rangle$ and $\alpha_j = e^{2\pi i \cdot (m_j/4k)}$. In this section we will assume that $m_j \neq 0$ for all $j \in [k]$

For $\ell \in \mathbb{Z}_{\geq 0}$, let

$$v_\ell = F\left(\frac{\ell v}{4k}\right) = \sum_{j=1}^k \lambda_j \alpha_j^\ell.$$

Note that $v_0 = F(\mathbf{0}) = \sum_j \lambda_j = 1$. Also note that we do not have access to $\alpha_1, \dots, \alpha_k$ and would like to recover m_1, m_2 given (noisy) access to $\{v_\ell\}_{0 \leq \ell \leq 2k-1}$.

Consider the generalized eigenvalue problem $(VD_\lambda V^\top, VD_\lambda D_\alpha V^\top)$ where

$$V = \begin{pmatrix} 1 & 1 & \cdots & 1 \\ \alpha_1 & \alpha_2 & \cdots & \alpha_k \\ \vdots & \vdots & \ddots & \vdots \\ \alpha_1^{k-1} & \alpha_2^{k-1} & \cdots & \alpha_k^{k-1} \end{pmatrix}, \quad D_\lambda = \text{diag}(\lambda), \quad D_\alpha = \text{diag}(\alpha).$$

The following standard facts are key to the matrix pencil method:

Observation 3.1. *The generalized eigenvalues of $(VD_\lambda V^\top, VD_\lambda D_\alpha V^\top)$ are exactly $\alpha_1, \dots, \alpha_k$.*

Observation 3.2.

$$VD_\lambda V^\top = \begin{pmatrix} v_0 & v_1 & \cdots & v_{k-1} \\ v_1 & v_2 & \cdots & v_k \\ \vdots & \vdots & \ddots & \vdots \\ v_{k-1} & v_k & \cdots & v_{2k-2} \end{pmatrix} \quad VD_\lambda D_\alpha V^\top = \begin{pmatrix} v_1 & v_2 & \cdots & v_k \\ v_2 & v_3 & \cdots & v_{k+1} \\ \vdots & \vdots & \ddots & \vdots \\ v_k & v_{k+1} & \cdots & v_{2k-1} \end{pmatrix}.$$

By Lemma 3.1, in reality we only have η'_ℓ -approximate access to each v_ℓ , where

$$\eta'_\ell \leq \frac{\eta}{\widehat{A}[\ell/4k]}, \quad (4)$$

so we must instead work with the generalized eigenvalue problem $(VD_\lambda V^\top + E, VD_\lambda D_\alpha V^\top + F)$, where the (i, j) -th entry of E (resp. F) is the noise η'_{i+j-2} (resp. η'_{i+j-1}) in the observation of v_{i+j-2} (resp. v_{i+j-1}).

If V is well-conditioned, one can apply standard perturbation bounds to argue that the solutions to this generalized eigenvalue problem are close to those of the original $(VD_\lambda V^\top, VD_\lambda D_\alpha V^\top)$. Moreover, given approximations $\widehat{\alpha}_1, \dots, \widehat{\alpha}_k$ to these generalized eigenvalues, we can find approximations $\widehat{\lambda}_1, \dots, \widehat{\lambda}_k$ to $\lambda_1, \dots, \lambda_k$ by solving the system of equations $\mathbf{v} = \widehat{V}\boldsymbol{\lambda}$, where $\mathbf{v} = (v_0, \dots, v_{k-1})$, $\boldsymbol{\lambda} = (\widehat{\lambda}_1, \dots, \widehat{\lambda}_k)$, and

$$\widehat{V} = \begin{pmatrix} 1 & 1 & \cdots & 1 \\ \widehat{\alpha}_1 & \widehat{\alpha}_2 & \cdots & \widehat{\alpha}_k \\ \vdots & \vdots & \ddots & \vdots \\ \widehat{\alpha}_1^{k-1} & \widehat{\alpha}_2^{k-1} & \cdots & \widehat{\alpha}_k^{k-1} \end{pmatrix}.$$

The formal specification of the matrix pencil method algorithm MODIFIEDMPM that we use is given in Algorithm 1.

The following theorem, implicit in the proof of Theorem 2.8 in [Moi15], makes the above reasoning precise. Henceforth, let $\kappa(\Delta')$ and $\sigma_{\min}(\Delta')$ respectively denote the condition number and minimum singular value of V when $\frac{m_i}{4k}, \frac{m_j}{4k}$ have minimum separation Δ' for all $i \neq j$, and define $\lambda_{\min} = \min_i \lambda_i$, $\lambda_{\max} = \max_i \lambda_i$.

Theorem 3.3 ([Moi15]). *Suppose $\frac{m_1}{4k}, \frac{m_2}{4k} \in [-1/4, 1/4]$ have separation at least Δ' and we are given η'_ℓ -close estimates to v_ℓ for $0 \leq \ell \leq 2k-1$.*

Define

$$\gamma = \frac{2\|\eta'\|_2}{\lambda_{\min}} \left(4\kappa(\Delta')^2 \cdot \frac{\lambda_{\max}}{\lambda_{\min}} + \frac{1}{\sigma_{\min}(\Delta')^2} \right) \quad \text{and} \quad \zeta = O\left(\frac{2\gamma\lambda_{\max} + \|\eta'\|_2}{\sigma_{\min}(\Delta' - 2\gamma)}\right)$$

Algorithm 1 MODIFIEDMPM

- 1: **Input:** $\omega \in \mathbb{S}^1$, η -approximate OTF oracle \mathcal{O}
- 2: **Output:** Estimates $(\widehat{\lambda}_1, \dots, \widehat{\lambda}_k)$ for the mixing weights and $(\widehat{m}_1, \dots, \widehat{m}_k)$ for the centers of ρ projected in direction ω
- 3: Define $\widehat{v}_0 = 1$.
- 4: For $0 \leq \ell \leq 2k - 1$: invoke \mathcal{O} on input $\frac{\ell\omega}{4k}$ to produce $u_\ell \in \mathbb{R}$. Compute $\widehat{v}_\ell \triangleq \frac{u_\ell}{A[\ell/4k]}$.
- 5: Form the matrices

$$X \triangleq \begin{pmatrix} \widehat{v}_0 & \cdots & \widehat{v}_{k-1} \\ \vdots & \ddots & \vdots \\ \widehat{v}_{k-1} & \cdots & \widehat{v}_{2k-2} \end{pmatrix} \quad Y \triangleq \begin{pmatrix} \widehat{v}_1 & \cdots & \widehat{v}_k \\ \vdots & \ddots & \vdots \\ \widehat{v}_k & \cdots & \widehat{v}_{2k-1} \end{pmatrix}$$

- 6: Solve the generalized eigenvalue problem (X, Y) to produce generalized eigenvalues $\widehat{\alpha}_1, \widehat{\alpha}_2$.
- 7: For $i = 1, 2$, let \widehat{m}_i be the argument of the projection of $\widehat{\alpha}_i$ onto the complex unit disk.
- 8: Form the matrix

$$\widehat{V} = \begin{pmatrix} 1 & 1 & \cdots & 1 \\ \widehat{\alpha}_1 & \widehat{\alpha}_2 & \cdots & \widehat{\alpha}_k \\ \vdots & \vdots & \ddots & \vdots \\ \widehat{\alpha}_1^{k-1} & \widehat{\alpha}_2^{k-1} & \cdots & \widehat{\alpha}_k^{k-1} \end{pmatrix}.$$

- 9: Solve for $\widehat{\lambda} = (\widehat{\lambda}_1, \dots, \widehat{\lambda}_k)$ such that $\widehat{V}\widehat{\lambda} = (\widehat{v}_0, \dots, \widehat{v}_{k-1})$.
 - 10: Output $\{\widehat{\lambda}_i\}_{i \in [k]}$ and $\{\widehat{m}_i\}_{i \in [k]}$.
-

Then if $\|E\| + \|F\| < \sigma_{\min}(\Delta')^2 \lambda_{\min}$ and $\gamma < \Delta'/4$, MODIFIEDMPM produces estimates $\{\widehat{\lambda}_i\}$ for the mixing weights and estimates $\{\widehat{m}_i\}$ for the projected centers such that for some permutation τ :

$$|m_i - \widehat{m}_{\tau(i)}| \leq 8\gamma \quad \text{and} \quad |\lambda_i - \widehat{\lambda}_i| \leq \zeta.$$

for all $i \in [k]$.

Note that the guarantees of Theorem 3.3 are stated in [Moi15] in terms of wraparound distance on the interval $[-1/2, 1/2]$, but because $\frac{m_j}{4k} \in [-1/4, 1/4]$ for all $j \in [k]$, $\frac{m_1}{4k}, \dots, \frac{m_k}{4k}$ have pairwise separation Δ' both in absolute and wraparound distance.

In other words, the output of MODIFIEDMPM converges to the true values for $\{\langle \mu_1, v \rangle\}_{j \in [k]}$ and $\{\lambda_j\}_{j \in [k]}$ at a rate polynomial in the noise rate, condition number of V , and relative intensity of the Airy disks, provided $\sigma_{\min}(\Delta')$ is inverse polynomially large and $\kappa(\Delta')$ is polynomially small in those parameters.

To complete the argument, we must establish these bounds on σ_{\min} and κ . Henceforth, let

$$\Delta' = \min_{i \neq j} \frac{m_i - m_j}{4k}.$$

Lemma 3.2. For any $k \geq 2$, we have that

$$\sigma_{\min}(\Delta')^2 \geq (\Delta'^k/k^2)^{k-1} \quad \text{and} \quad \kappa(\Delta')^2 \leq k^{2k-1}/\Delta'^{k(k-1)}$$

Proof. First note that $\sigma_{\max}(\Delta')^2 \leq k^2$. Indeed because the entries of V all have absolute value at

most 1, we conclude that for any $v \in \mathbb{S}^{k-1}$ and any row index $j \in [k]$,

$$\langle V_j, v \rangle^2 \leq \left(\sum_{i=1}^k |v_i| \right)^2 \leq k.$$

On the other hand, we also have that

$$\prod_{i=1}^k \sigma_i(V) = |\det(V)| = \prod_{1 \leq i < j \leq k} |\alpha_i - \alpha_j| \leq \left| e^{2\pi i \Delta'} - 1 \right|^{\binom{k}{2}} = (2 - 2 \cos(\Delta'))^{\binom{k}{2}/2} \geq \Delta'^{k(k-1)/2},$$

where in the first step we used the standard fact that the absolute value of the determinant of a square matrix is equal to the product of its singular values, in the second step we used the standard identity for the determinant of a Vandermonde matrix, in the third step we used the angular separation of the α_i 's, and in the final step we used the elementary inequality $\cos(\Delta') \leq 1 - \Delta'^2/2$. We may thus naively lower bound $\sigma_{\min}(V)$ by $\frac{\Delta'^{k(k-1)/2}}{k^{k-1}}$, from which the lemma follows. \square

This yields the following consequence for MODIFIEDMPM.

Corollary 3.1. *Given $\omega \in \mathbb{S}^1$ and access to an η -approximate OTF oracle \mathcal{O} , if the projected centers $m_j = \langle \mu_j, v \rangle$ satisfy $|m_i - m_j| \leq 4k \cdot \Delta'$ for all $i \neq j$ for some $0 < \Delta' \leq 1/16$, then there exists a constant $c_2 > 0$ such that provided that*

$$\eta \leq c_2 \lambda_{\min}^2 \Delta'^{k^2} \cdot k^{-2k-1/2}, \quad (5)$$

then MODIFIEDMPM produces estimates $\{\hat{\lambda}_i\}$ for the mixing weights and estimates $\{\hat{m}_i\}$ for the projected centers such that for some permutation τ :

$$|m_i - \hat{m}_{\tau(i)}| \leq O\left(\frac{k^{2k+1/2} \cdot \eta}{\lambda_{\min}^2 \Delta'^{k(k-1)}}\right) \quad \text{and} \quad |\lambda_i - \hat{\lambda}_{\tau(i)}| \leq O\left(\frac{k^{3k-1/2} \cdot \eta}{\lambda_{\min}^2 \Delta'^{3k(k-1)/2}}\right)$$

for all $i \in [k]$.

Proof. From Lemma 3.2, we have that $\sigma_{\min}(\Delta')^2 \geq (\Delta'^k/k^2)^{k-1}$. Then because $\kappa(\Delta')^2 \leq k^2/\sigma_{\min}(\Delta')^2$, we would like to conclude by Theorem 3.3 that $|m_i - \hat{m}_{\tau(i)}| \leq 8\gamma$, where

$$\gamma = O\left(\frac{\|\eta'\|_2 \cdot k^2}{\lambda_{\min}^2 \cdot \sigma_{\min}(\Delta')^2}\right) = O\left(\frac{\|\eta'\|_2 \cdot k^2}{\lambda_{\min}^2 \cdot (\Delta'^k/k^2)^{k-1}}\right) = O\left(\frac{k^{2k+1/2} \cdot \eta}{\lambda_{\min}^2 \Delta'^{k(k-1)}}\right),$$

where in the last step we use that the vector η' has length $O(k)$ and satisfies $\|\eta'\|_{\infty} \leq O(\eta)$ by (4). To do so, we just need to verify that $\|E\| + \|F\| < \sigma_{\min}(\Delta')^2 \lambda_{\min}$ and $\gamma < \Delta'/4$. The latter clearly follows from the bound (5) for sufficiently small c_2 . For the former, note that

$$\|E\|_2 \leq \|E\|_F \leq \sqrt{k} \cdot \sqrt{\eta_1^2 + \dots + \eta_{2k-1}^2} \leq \eta \sqrt{k} \cdot \sqrt{\sum_{\ell=1}^{2k-1} \frac{1}{\hat{A}[\ell/4k]}} \leq O(\eta \cdot k),$$

where the last step follows by the fact that $\hat{A}[\ell/4k] \geq \hat{A}[1/2] \geq \Omega(1)$. The same bound holds for $\|F\|_2$. Recalling that $\sigma_{\min}(\Delta')^2 \geq (\Delta'^k/k^2)^{k-1}$, it is enough for $\eta \leq O(\Delta'^k/k^2)^{k-1} \lambda_{\min}/k$, which certainly holds for η satisfying (5), for c_2 sufficiently small.

Finally, Theorem 3.3 also implies that $|\lambda_i - \hat{\lambda}_i| \leq \zeta$, where

$$\zeta \leq O\left(\frac{\gamma + k^{1/2}\eta}{\sigma_{\min}(\Delta' - 2\gamma)}\right) \leq O\left(\frac{k^{2k+1/2} \cdot \eta}{\lambda_{\min}^2 \Delta'^{k(k-1)} \cdot (\Delta'^{k(k-1)/2}/k^{k-1})}\right) = O\left(\frac{k^{3k-1/2} \cdot \eta}{\lambda_{\min}^2 \Delta'^{3k(k-1)/2}}\right)$$

as claimed. \square

3.2.2 Combining Directions

We can run MODIFIEDMPM to approximately recover $\{\langle \boldsymbol{\mu}_j, \omega_1 \rangle\}_{j \in [k]}$ and $\{\langle \boldsymbol{\mu}_j, \omega_2 \rangle\}_{j \in [k]}$ for two randomly chosen directions $\omega_1, \omega_2 \in \mathbb{S}^1$. As these directions are random, with high probability we can combine these estimates to obtain an accurate estimate of $\{\boldsymbol{\mu}_j\}_{j \in [k]}$. One subtlety is that the estimates $\{\hat{m}_j\}$ and $\{\hat{m}'_j\}$ output by MODIFIEDMPM for the centers projected in directions ω_1 and ω_2 respectively need not be aligned, that is we only know that there exists some permutation τ for which $\hat{m}_j = \hat{m}'_{\tau(j)}$ for $j \in [k]$.

We first show a “pairing lemma” stating that if ω_1 is chosen randomly and ω_2 is chosen to be close to ω_1 , then if one sorts the centers $\boldsymbol{\mu}_1, \dots, \boldsymbol{\mu}_k$, first in terms of their projections in the ω_1 direction, and then in terms of their projections in the ω_2 direction, the corresponding elements in these two sorted sequences will correspond to the same centers.

We require the following elementary fact.

Lemma 3.3. *For $\boldsymbol{\mu} \in \mathbb{R}^2$ a unit vector and $\omega \in \mathbb{R}^2$ a random unit vector, $\Pr_{\omega}[\langle \boldsymbol{\mu}, \omega \rangle \leq \sin \theta] = 2\theta/\pi$ for all $0 \leq \theta \leq \pi/2$.*

Lemma 3.4. *Fix an arbitrary $0 < \theta \leq \pi/2$ and let $v = \frac{\Delta \sin \theta}{8}$. Let $\omega_1 \in \mathbb{R}^2$ be a random unit vector, and let $\omega_2 \in \mathbb{R}^2$ be either of the two unit vectors for which $\|\omega_1 - \omega_2\|_2 = v$. For every $i \in [k]$, define $m_i \triangleq \langle \boldsymbol{\mu}_i, \omega_1 \rangle$ and $m'_i \triangleq \langle \boldsymbol{\mu}_i, \omega_2 \rangle$, and let $\hat{m}_i, \hat{m}'_i \in \mathbb{R}$ be any numbers for which $\|\hat{m}_i - m_i\|_2, \|\hat{m}'_i - m'_i\|_2 \leq 2v$.*

Then with probability at least $1 - \frac{k(k-1)\theta}{\pi}$, for every $i \neq j$ the following are equivalent: I) $m_i > m_j$, II) $m'_i > m'_j$, III) $\hat{m}_i > \hat{m}_j$, and IV) $\hat{m}'_i > \hat{m}'_j$.

Proof. By Lemma 3.3 and a union bound we have that with probability $1 - \frac{k(k-1)\theta}{\pi}$, $|m_i - m_j| > \Delta \sin \theta$ for all $i \neq j$. Fix any $i \neq j$ and suppose that $m_i > m_j$. Then by triangle inequality and Cauchy-Schwarz, we have that

$$m'_i - m'_j = \langle \boldsymbol{\mu}_i - \boldsymbol{\mu}_j, \omega_2 \rangle = \langle \boldsymbol{\mu}_i - \boldsymbol{\mu}_j, \omega_1 \rangle + \langle \boldsymbol{\mu}_i - \boldsymbol{\mu}_j, \omega_2 - \omega_1 \rangle \geq \Delta \sin \theta - 4v > 0,$$

where the final inequality follows by the definition of v . So I) implies II) and by symmetry we can show II) implies I). We also have that

$$\hat{m}_i - \hat{m}_j \geq (m_i - m_j) - 4v > 0,$$

so I) implies III) and by symmetry we can show II) implies IV).

It is enough to show that III) implies I). Suppose $\hat{m}_i > \hat{m}_j$. Then

$$m_i - m_j \geq (\hat{m}_i - \hat{m}_j) - 4v > -\frac{1}{2}\Delta \sin \theta > -\Delta \sin \theta,$$

so it must be the case that $m_i - m_j > 0$ given that $|m_i - m_j| > \Delta \sin \theta$. \square

We now show that we can combine these projected center estimates to approximately recover the two-dimensional centers by solving a linear system. The specification of this algorithm, which we call PRECONSOLIDATE, is given in Algorithm 2.

Lemma 3.5. *Let $\xi > 0$. Let the parameters θ, v and the random vectors ω_1, ω_2 be as in Lemma 3.4. Suppose $\{\hat{m}_i\}_{i \in [k]}$ and $\{\hat{m}'_i\}_{i \in [k]}$ are collections of numbers for which there exist permutations $\tau_1, \tau_2 \in \mathbb{S}_k$ for which*

$$|\langle \omega_1, \boldsymbol{\mu}_i \rangle - \hat{m}_{\tau_1(i)}| \leq \xi \quad \text{and} \quad |\langle \omega_2, \boldsymbol{\mu}_i \rangle - \hat{m}'_{\tau_2(i)}| \leq \xi$$

Algorithm 2 PRECONSOLIDATE

- 1: **Input:** Directions $\omega_1, \omega_2 \in \mathbb{S}^1$ and estimates $\{\hat{\lambda}_i\}, \{\hat{m}_i\}$ and $\{\hat{\lambda}'_i\}, \{\hat{m}'_i\}$ for the parameters of ρ projected in the directions ω_1 and ω_2 respectively
- 2: **Output:** An estimate of the form $(\{\tilde{\lambda}_i\}, \{\tilde{\mu}_i\})$ for the parameters of ρ .
- 3: **for** $i \in [k]$ **do**
- 4: Let $\ell, \ell' \in [k]$ be the indices for which \hat{m}_ℓ and $\hat{m}'_{\ell'}$ are the i -th largest in $\{\hat{m}_j\}_{j \in [k]}$ and $\{\hat{m}'_j\}_{j \in [k]}$ respectively.
- 5: Define a formal vector-valued variable $\mathbf{v}^{(i)} \in \mathbb{R}^2$ and solve the linear system

$$\begin{aligned}\langle \omega_1, \mathbf{v}^{(i)} \rangle &= \hat{m}_\ell \\ \langle \omega_2, \mathbf{v}^{(i)} \rangle &= \hat{m}'_{\ell'}.\end{aligned}$$

- 6: **Output** $(\{\hat{\lambda}_i\}_{i \in [k]}, \{\mathbf{v}^{(i)}\}_{i \in [k]})$.
-

for all $i \in [k]$.

Then for any estimates $\{\hat{\lambda}_i\}_{i \in [k]}$ and $\{\hat{\lambda}'_i\}_{i \in [k]}$, with probability at least $1 - \frac{k(k-1)\theta}{\pi}$ we have that the output $(\{\tilde{\lambda}_i\}, \{\tilde{\mu}_i\})$ of PRECONSOLIDATE($\omega_1, \omega_2, \{\hat{\lambda}_i\}, \{\hat{m}_i\}, \{\hat{\lambda}'_i\}, \{\hat{m}'_i\}$) satisfies

$$\|\boldsymbol{\mu}_i - \tilde{\boldsymbol{\mu}}_{\tau(i)}\|_2 \leq \frac{\xi}{v\sqrt{1-v^2/4}}$$

for some permutation $\tau \in \mathbb{S}_k$.

Proof. Condition on the event of Lemma 3.4 occurring, which happens with probability at least $1 - \frac{k(k-1)\theta}{\pi}$. This event implies that there is a permutation $\tau \in \mathbb{S}_k$ such that for every $i \in [k]$ in the loop of PRECONSOLIDATE, the indices ℓ, ℓ' in that iteration are such that \hat{m}_ℓ and $\hat{m}'_{\ell'}$ are ξ -close estimates for the projections of $\boldsymbol{\mu}_{\tau(i)}$ in the directions ω_1 and ω_2 respectively. In other words, $\tau_1(\tau(i)) = \ell$ and $\tau_2(\tau(i)) = \ell'$.

Let $A \in \mathbb{R}^{2 \times 2}$ be the matrix with rows consisting of ω_1 and ω_2 . We conclude that

$$\|\boldsymbol{\mu}_{\tau(i)} - \mathbf{v}^{(i)}\|_2 = \|A^{-1} \cdot ((\hat{m}_\ell, \hat{m}'_{\ell'}) - (\langle \omega_1, \boldsymbol{\mu}_{\tau(i)} \rangle, \langle \omega_2, \boldsymbol{\mu}_{\tau(i)} \rangle))\|_2 \leq \sigma_{\min}(A) \cdot \xi,$$

so it remains to bound $\sigma_{\min}(A)$. Without loss of generality we may assume $\omega_1 = (1, 0)$ and $\omega_2 = (x, \sqrt{1-x^2})$ for $x \triangleq 1 - v^2/2$, in which case $\sigma_{\min}(A) = v\sqrt{1-v^2/4}$, and the claim follows. \square

Finally, we show how to boost the success probability via the following naive clustering-based algorithm SELECT (Algorithm 3), whose guarantees we establish below.

We can now give the full specification of our algorithm LEARNAIRYDISKS (see Algorithm 4).

Lemma 3.6. *Let ρ be a Δ -separated superposition of k Airy disks. For any $\epsilon_1, \epsilon_2, \delta > 0$, let*

$$\eta = O\left(\left(\frac{\Delta}{4k}\right)^{O(k^2)} \cdot \lambda_{\min}^2\right) \cdot \min\{\epsilon_1/M, \epsilon_2\}. \quad (6)$$

Without loss of generality suppose $\epsilon_1 < 3\Delta/8$. Then the output $(\lambda_1^, \lambda_2^*, \boldsymbol{\mu}_1^*, \boldsymbol{\mu}_2^*)$ of LEARNAIRYDISKS, given $\epsilon_1, \epsilon_2, \delta$ and access to an η -approximate, $O(\log(1/\delta))$ -query OTF oracle \mathcal{O} for ρ , satisfies*

$$\|\boldsymbol{\mu}_i - \boldsymbol{\mu}_{\tau(i)}^*\|_2 \leq \epsilon_1 \quad \text{and} \quad |\lambda_i - \lambda_{\tau(i)}| \leq \epsilon_2$$

Algorithm 3 SELECT

- 1: **Input:** Accuracy parameters ϵ'_1, ϵ'_2 , and list \mathcal{L} consisting of T candidate estimates for the parameters of ρ , each of the form $\left(\{\tilde{\lambda}_i^t\}_{i \in [k]}, \{\tilde{\mu}_i^t\}_{i \in [k]}\right)$ for $t \in [T]$, such that for at least $1 - \frac{1}{2k}$ fraction of all $t \in [T]$, $\left(\{\tilde{\lambda}_i^t\}_{i \in [k]}, \{\tilde{\mu}_i^t\}_{i \in [k]}\right)$ is an $(\epsilon'_1, \epsilon'_2)$ -accurate estimate of the parameters of ρ .
 - 2: **Output:** A $(3\epsilon'_1, \epsilon'_2)$ -accurate estimate of the parameters of ρ
 - 3: Define $\mathcal{S} = T \times [k]$.
 - 4: Form the graph $G = (V, E)$ whose vertices consist of all (t, i) for which $\tilde{\mu}_i^t \in \mathcal{S}$ is $2\epsilon'_1$ -close to at least $2T/3$ other points in \mathcal{S} , with edges between any $(t, i), (t', i')$ for which $\|\tilde{\mu}_i^t - \tilde{\mu}_{i'}^{t'}\| > 6\epsilon'_1$.
 - 5: G is k -partite. Denote the parts by $V^{(1)}, \dots, V^{(k)} \subset V$.
 - 6: **for** $j \in [k]$ **do**
 - 7: Form the set $\{\tilde{\lambda}_i^t\}_{(t,i) \in V^{(j)}}$ and let λ_j^* be the median of this set, corresponding to some $(t_j, i_j) \in \mathcal{S}$.
 - 8: Define $\mu_j^* \triangleq \tilde{\mu}_{i_j}^{t_j}$.
 - 9: Output $\left(\{\lambda_j^*\}_{j \in [k]}, \{\mu_j^*\}_{j \in [k]}\right)$.
-

Algorithm 4 LEARN AIRY DISKS

- 1: **Input:** Error parameters ϵ_1, ϵ_2 , confidence parameter δ , access to η -approximate, $O(\log 1/\delta)$ -query OTF oracle
 - 2: **Output:** With probability at least $1 - \delta$, an (ϵ_1, ϵ_2) -accurate estimate $(\{\tilde{\lambda}_i\}, \{\tilde{\mu}_i\})$ for the parameters of ρ .
 - 3: Initialize a list \mathcal{L} of candidate estimates for the parameters of ρ .
 - 4: Set $\theta \triangleq \frac{\pi}{3k^2(k-1)}$.
 - 5: Set η according to (6).
 - 6: **for** $T = \Omega(\log(1/\delta))$ iterations **do**
 - 7: Sample a random unit vector $\omega_1 \in \mathbb{S}^1$ and let ω_2 be either of the two unit vectors for which $\|\omega_1 - \omega_2\|_2 = \Delta \sin \theta / 8$ (see Lemma 3.4).
 - 8: Run MODIFIEDMPM(ω_1, \mathcal{O}) and MODIFIEDMPM(ω_2, \mathcal{O}) to obtain estimates $\{\hat{\lambda}_i\}, \{\hat{m}_i\}$ and $\{\tilde{\lambda}_i\}, \{\tilde{m}_i\}$ for the parameters of ρ projected in the directions ω_1, ω_2 respectively.
 - 9: Let $\{\tilde{\lambda}_i^t\}, \{\tilde{\mu}_i^t\}$ be the estimates output by PRECONSOLIDATE($\omega_1, \omega_2, \{\hat{\lambda}_i\}, \{\hat{m}_i\}, \{\tilde{\lambda}_i\}, \{\tilde{m}_i\}$). Append these to \mathcal{L} .
 - 10: Output what is returned by SELECT($\mathcal{L}, \epsilon_1/3, \epsilon_2$).
-

for some permutation τ with probability at least $1 - \delta$. Furthermore, the runtime of LEARNAIRYDISKS is dominated by the time it takes to invoke the OTF oracle $O(\log(1/\delta))$ times.

Proof. Suppose we are given a valid η -approximate OTF oracle \mathcal{O} . By taking $\theta = \frac{\pi}{3k^2(k-1)}$ and invoking Lemmas 3.1 and 3.5, we ensure that a single run of PRECONSOLIDATE in an iteration of the loop in Step 6 of LEARNAIRYDISKS will yield, with probability at least $1 - \frac{1}{3k}$, an $(\epsilon'_1, \epsilon'_2)$ -accurate estimate, where

$$\epsilon'_1 = \frac{8}{\Delta \sin \theta} \cdot O\left(\frac{k^{2k+1/2} \cdot \eta}{\lambda_{\min}^2 \left(\frac{\Delta \sin \theta}{4k}\right)^{k(k-1)}}\right) \quad \text{and} \quad \epsilon'_2 = O\left(\frac{k^{3k-1/2} \cdot \eta}{\lambda_{\min}^2 \left(\frac{\Delta \sin \theta}{4k}\right)^{3k(k-1)/2}}\right).$$

In this case we say that such an iteration of the loop in LEARNAIRYDISKS “succeeds.” Note that if we take

$$\eta = O\left(\min\left\{\epsilon_1 \cdot \frac{\Delta \sin \theta}{8} \cdot \frac{\lambda_{\min}^2 \left(\frac{\Delta \sin \theta}{4k}\right)^{k(k-1)}}{k^{2k+1/2}}, \epsilon_2 \cdot \frac{\lambda_{\min}^2 \left(\frac{\Delta \sin \theta}{4k}\right)^{3k(k-1)/2}}{k^{3k-1/2}}\right\}\right),$$

then we can ensure that $\epsilon'_1 = \epsilon_1/3$ and $\epsilon'_2 = \epsilon_2$. The bound in (6) then follows from the elementary inequality $\sin \theta \geq \theta/2$ for $0 \leq \theta \leq 1$, together with our choice of $\theta = \frac{\pi}{3k^2(k-1)}$.

Each iteration of the loop in Step 6 of LEARNAIRYDISKS individually succeeds with probability at least $1 - \frac{1}{3k}$. So by a Chernoff bound, by taking $T = \Omega(\log(1/\delta))$, we conclude that with probability at least $1 - \delta$, at least $1 - \frac{1}{2k}$ fraction of these iterations will succeed. So of the $k \cdot T$ elements in \mathcal{S} , at most $T/2$ correspond to failed iterations.

Now note that all (t, i) for which t corresponds to a successful iteration will be $2\epsilon'_1$ -close to at least $k \cdot T - T/2 > 2T/3$ points. In particular, any such (t, i) will be among the vertices V of G in Algorithm 3. Conversely, for any $(t, i) \in V$, $\tilde{\mu}_i^t$ is by definition $2\epsilon'_1$ -close to at least $2T/3$ points and there are at most $T/2 < 2T/3$ points which do not correspond to successful iterations. In particular, at least one of the points that $\tilde{\mu}_i^t$ is close to will correspond to a successful iteration, so by the triangle inequality $\|\tilde{\mu}_i^t - \mu_j\| \leq 3\epsilon'_1$ for some choice of $j \in [k]$.

Observe that G is k -partite because every vertex in V is $3\epsilon'_1$ -close to some center of ρ , but two vertices which are $3\epsilon'_1$ -close to μ_i and μ_j respectively for $i \neq j$ must be distance at least $\Delta - 6\epsilon'_1 > 2\epsilon'_1$ apart. We conclude that with high probability, SELECT will output $3\epsilon'_1 = \epsilon_1$ -accurate estimates for the centers of ρ .

It remains to show that λ_1^*, λ_2^* are ϵ_2 -accurate estimates for the mixing weights. We know the estimates $\tilde{\lambda}_i^t$ corresponding to successful iterations t and center μ_i lie in $\{\tilde{\lambda}_i^t\}_{(t,i) \in V^{(\ell)}}$ for some ℓ . Then $\{\tilde{\lambda}_i^t\}_{(t,i) \in V^{(\ell)}}$ contains at least $(1 - \frac{1}{2k})T > 2T/3$ values that are ϵ'_2 -close to λ_1 , and at most $T/2 < 2T/3$ other values. Call these values “good” and “bad” respectively. Either the median is good, in which case we are done, or the median is bad, in which case because there are strictly more good values than bad values, the median must be upper and lower bounded by good values, in which case we are still done.

Finally, note that in each iteration of the main loop of LEARNAIRYDISKS, \mathcal{O} is invoked exactly six times. Furthermore, other than these invocations of \mathcal{O} , the remaining steps of LEARNAIRYDISKS all require constant time. So the runtime of LEARNAIRYDISKS is indeed dominated by the $O(\log(1/\delta))$ calls to \mathcal{O} . \square

3.3 Learning Airy Disks Above the Diffraction Limit

In this subsection we present the proof of Theorem 3.2. Recall that we are assuming that $\sigma = 1/\pi$ and $\Delta > \gamma_{\text{res}}$, where γ_{res} is defined in (2). Let $c \triangleq \frac{1}{2}(\Delta + \gamma_{\text{res}})$ and define $R \triangleq \frac{\gamma_{\text{res}}}{2c}$ and $r \triangleq 1/2 - R$.

We will use the following Algorithm 5 that we call TENSORRESOLVE. While this is only a slight modification of the tensor decomposition algorithm of [HK15] for high-dimensional superresolution, our analysis is novel and obtains sharper results in low dimensions by using certain extremal functions [Gon18, HV⁺96, CCLM17] arising in the study of de Branges spaces (see Theorem 3.4).

Algorithm 5 TENSORRESOLVE

- 1: **Input:** Error parameters ϵ_1, ϵ_2 , confidence parameter δ , access to η -approximate, $\Theta\left(\frac{k^2 \log(1/\delta)}{(\Delta - \gamma_{\text{res}})\wedge 1}\right)$ -query OTF oracle
 - 2: **Output:** With probability at least $1 - \delta$, an (ϵ_1, ϵ_2) -accurate estimate $(\{\tilde{\lambda}_i\}, \{\tilde{\mu}_i\})$ for the parameters of ρ , provided the separation is sufficiently above the diffraction limit (see Lemma 3.12)
 - 3: Define $R = \gamma_{\text{res}}/2c$ and $r \triangleq 1/2 - R$.
 - 4: Sample $\omega^{(1)}, \dots, \omega^{(m)}$ i.i.d. from the uniform distribution over $B^2(R)$. Also define $\omega^{(m+1)} = (1, 0)$, $\omega^{(m+2)} = (0, 1)$, and $\omega^{(m+3)} = (0, 0)$. Define $m' \triangleq m + 3$
 - 5: Sample v uniformly from \mathbb{S}^1 and define $v^{(1)} = r \cdot v$, $v^{(2)} = 2r \cdot v$, and $v^{(3)} = 0$.
 - 6: Define $\xi_{a,b,i} \triangleq \omega^{(a)} + \omega^{(b)} + v^{(i)}$ for every $a, b \in [m']$, $i \in [3]$. Query the OTF oracle at $\{\xi_{a,b,i}\}$ to obtain numbers $\{u_{a,b,i}\}$. Construct the tensor $\tilde{\mathbf{T}} \in \mathbb{C}^{m' \times m' \times 3}$ given by $\tilde{\mathbf{T}}_{a,b,i} = u_{a,b,i}/\widehat{A}[\xi_{a,b,i}]$.
 - 7: Let $\hat{V} \in \mathbb{R}^{m' \times k}$ be the output of JENNRICH($\tilde{\mathbf{T}}$) (defined in Algorithm 7). Divide each column \hat{V}^j by a factor of $\hat{V}_{m,j}$.
 - 8: For each $j \in [k]$, $i \in [2]$, let $\hat{\mu}_j \in \mathbb{R}^2$ have i -th entry equal to the argument of the projection of $\hat{V}_{m+i,j}$ onto the complex disk.
 - 9: Query the OTF oracle at frequencies $\{\omega^{(a)}\}_{a \in [m']}$ to get numbers $\{u'_a\}_{a \in [m']}$ and form the vector $\hat{b} \in \mathbb{R}^{m'}$ whose a -th entry is $u'_a/\widehat{A}[\omega^{(a)}]$ for every $a \in [m']$.
 - 10: Let $\hat{\lambda} \in \mathbb{R}^k = \arg\min_{\lambda} \|\hat{V}\lambda - \hat{b}\|_2$.
 - 11: Return $(\hat{\lambda}_1, \dots, \hat{\lambda}_k)$ and $(\hat{\mu}_1, \dots, \hat{\mu}_k)$.
-

Using the notation of TENSORRESOLVE, define the tensor $\mathbf{T} \in \mathbb{C}^{m' \times m' \times 3}$ given by

$$\mathbf{T}_{a,b,i} = \sum_{j=1}^k \lambda_j e^{-2\pi i \langle \mu_j, \omega^{(a)} + \omega^{(b)} + v^{(i)} \rangle}$$

and note that it admits a low-rank decomposition as

$$\mathbf{T} = \sum_{j=1}^k V^j \otimes V^j \otimes (W^j D_\lambda), \quad (7)$$

where D_λ is the diagonal matrix whose entries consist of the mixing weights $\{\lambda_j\}$ and, for every $j \in [k]$, $W^j = (e^{-2\pi i \langle \mu_j, v^{(1)} \rangle}, e^{-2\pi i \langle \mu_j, v^{(2)} \rangle}, e^{-2\pi i \langle \mu_j, v^{(3)} \rangle})$ and $V^j = (e^{-2\pi i \langle \mu_j, \omega^{(1)} \rangle}, \dots, e^{-2\pi i \langle \mu_j, \omega^{(m')} \rangle})$. Let $V \in \mathbb{R}^{m' \times k}$ denote the matrix whose j -th column is V^j .

Note that by our choice of r, R and triangle inequality, we have that $\|\omega^{(a)} + \omega^{(b)} + v^{(i)}\|_2 \leq r + 2R = 1 - \frac{c - \gamma_{\text{res}}}{2c} < 1$ for any entry index a, b, i . So if $\{u_{a,b,i}\}$ are the numbers obtained from an η -approximate, $(m + 3)$ -query OTF oracle as in Algorithm 5, and $\tilde{\mathbf{T}}$ is constructed as in Step 6 of TENSORRESOLVE, then by Lemma 3.1 we have that

$$|\mathbf{T}_{a,b,i} - \tilde{\mathbf{T}}_{a,b,i}| \leq \frac{\eta}{\widehat{A}[1 - \frac{c - \gamma_{\text{res}}}{2c}]} \leq \eta \cdot \left(\frac{c - \gamma_{\text{res}}}{2c}\right)^2,$$

where the last step follows by Fact 2.

The following is a consequence of the stability of Jennrich's algorithm.

Lemma 3.7. [e.g. [HK15], Lemma 3.5] For any $\epsilon, \delta > 0$, suppose $|\mathbf{T}_{a,b,i} - \tilde{\mathbf{T}}_{a,b,i}| \leq \eta'$ for $\eta' \triangleq O\left(\frac{(c-\gamma_{\text{res}})\delta\Delta\lambda_{\min}^2}{k^{5/2}m^{3/2}\kappa(V)^5} \cdot \epsilon\right)$, and let $\hat{V} = \text{JENNRICH}(\tilde{\mathbf{T}})$ (Algorithm 7). Then with probability at least $1 - \delta$ over the randomness of $v^{(1)}$, there exists permutation matrix Π such that $\|\hat{V} - V\Pi\|_F \leq \epsilon$ for all $j \in [k]$.

The setting of parameters in [HK15] is slightly different from ours, so we provide a self-contained proof of Lemma 3.7 in Appendix D.

We will also need the following basic lemma about the stability of solving for $\hat{\lambda}$ in Step 10 in TENSORRESOLVE.

Lemma 3.8. For any $\epsilon, \epsilon' > 0$, if $\lambda \in \mathbb{R}^k$ satisfies $V\lambda = b$ for some $V \in \mathbb{R}^{m' \times k}$ and $b \in \mathbb{R}^{m'}$, and furthermore \hat{V}, \hat{b} satisfy $\|V - \hat{V}\|_2 \leq \epsilon$ and $\|b - \hat{b}\|_2 \leq \epsilon'$, then $\hat{\lambda} \triangleq \text{argmin}_{\hat{\lambda}} \|\hat{V}\hat{\lambda} - \hat{b}\|_2$ satisfies $\|\lambda - \hat{\lambda}\|_2 \leq \frac{2\epsilon\|\lambda\|_2 + 2\epsilon'}{\sigma_{\min}(V) - \epsilon}$.

Proof. Note that

$$\|\hat{V}\lambda - \hat{b}\|_2 \leq \|(\hat{V} - V)\lambda\|_2 + \|\hat{b} - b\|_2 \leq \epsilon\|\lambda\|_2 + \epsilon'.$$

By triangle inequality and definition of $\hat{\lambda}$, $\|\hat{V}(\hat{\lambda} - \lambda)\|_2 \leq 2\epsilon\|\lambda\|_2 + 2\epsilon'$, so $\|\hat{\lambda} - \lambda\|_2 \leq \frac{2\epsilon\|\lambda\|_2 + 2\epsilon'}{\sigma_{\min}(\hat{V})}$. The lemma follows because $\sigma_{\min}(V') \geq \sigma_{\min}(V) - \epsilon$. \square

It remains to show the following condition number bound.

Lemma 3.9. For any $\delta > 0$, if $m = \Theta\left(\frac{k^2 \log(1/\delta)}{(\Delta - \gamma_{\text{res}}) \wedge 1}\right)$, then $\kappa(V) \leq O\left(k \vee \frac{k}{\sqrt{\Delta - \gamma_{\text{res}}}}\right)$ and $\sigma_{\min}(V) \geq \Omega(k^2 \log(1/\delta))$ with probability at least $1 - \delta$.

Proof. Let $V^* \in \mathbb{R}^{m \times k}$ denote the submatrix given by the first m rows of V . We will need the following basic lemma from [HK15] relating the condition number of V^* to that of V :

Lemma 3.10 ([HK15], Lemma 3.8). $\kappa(V) \leq \sqrt{2k} \cdot \kappa(V^*)$.

The primary technical component of this section is to upper bound $\kappa(V^*)$. First, note that given any $\lambda \in \mathbb{C}^{k-1}$, we have that

$$\lambda^\dagger V^{*\dagger} V^* \lambda = \sum_{i=1}^m |\langle \lambda, V_i^* \rangle|^2 = \sum_{i=1}^m \left| \sum_{j=1}^k \lambda_j e^{-2\pi i \langle \mu_j, \omega^{(i)} \rangle} \right|^2.$$

As each $\omega^{(i)}$ is an independent draw from the uniform distribution over \mathbb{S}^1 , we have that

$$\mathbb{E}_{\omega^{(1)}, \dots, \omega^{(m)}} [\lambda^\dagger V^{*\dagger} V^* \lambda] = m \int_{B^2(R)} \left| \sum_{j=1}^k \lambda_j e^{-2\pi i \langle \mu_j, \omega \rangle} \right|^2 d\psi(\omega),$$

where $d\psi(\omega)$ is the uniform measure over $B^2(R)$. Furthermore, for any $\omega \in B^2(R)$ and $i \in [m]$, we have that

$$0 \leq |\langle \lambda, V_i^* \rangle|^2 \leq \|\lambda\|_1^2 \leq k \cdot \|\lambda\|_2^2. \quad (8)$$

So by Chernoff applied to the random variables $|\langle \lambda, V_1^* \rangle|^2, \dots, |\langle \lambda, V_m^* \rangle|^2$,

$$\Pr \left[\left| \lambda^\dagger V^{*\dagger} V^* \lambda - \mathbb{E}_{\omega^{(1)}, \dots, \omega^{(m)}} [\lambda^\dagger V^{*\dagger} V^* \lambda] \right| > \sqrt{mkt} \cdot \|\lambda\|_2^2 \right] \leq 2e^{-t/2} \quad \forall t > 0. \quad (9)$$

Lemma 3.11 below allows us to bound the expectation term. Taking $t = O(\sqrt{\log 1/\delta})$ and $m = \Theta\left(\frac{k^2 \log(1/\delta)}{(\Delta - \gamma_{\text{res}}) \wedge 1}\right)$ in (9) and applying Lemma 3.11, we conclude that with probability at least $1 - \delta$,

$$\Omega(m) \cdot \{(\Delta - \gamma_{\text{res}}) \wedge 1\} \cdot \|\lambda\|_2^2 \leq \lambda^\dagger V^{*\dagger} V^* \lambda \leq O(m) \cdot (k + \{(\Delta - \gamma_{\text{res}}) \wedge 1\}) \cdot \|\lambda\|_2^2,$$

from which it follows that with this probability, $\kappa(V^*) \leq O\left(\frac{k}{(\Delta - \gamma_{\text{res}}) \wedge 1}\right)^{1/2}$, from which the lemma follows by Lemma 3.10. \square

It remains to show Lemma 3.11 below, the key technical ingredient of this section. We will require the following special case of a result of [Gon18], which essentially follows from results of [CCLM17, HV⁺96]. This can be thought of as the high-dimensional generalization of the well-known Beurling-Selberg minorant (see, e.g., [Vaa85] for a discussion of the one-dimensional case).

Theorem 3.4 ([Gon18], Theorem 1). *For any $d \in \mathcal{N}$ and $\frac{j_{d/2-1,1}}{\pi} < r < \frac{j_{d/2,1}}{\pi}$, there exists a function $M \in L^1(\mathbb{R}^d)$ whose Fourier transform is supported in $B^d(r)$, and which satisfies $M(x) \leq \mathbb{1}[x \in B^d(1)]$ for all $x \in \mathbb{R}^d$ and $\widehat{M}[0] = \frac{(2/r)^d}{|\mathbb{S}^{d-1}|} \cdot \frac{C(d,r)}{1+C(d,r)/d}$, where $|\mathbb{S}^{d-1}|$ denotes the surface area of \mathbb{S}^{d-1} and $C(r, d) \triangleq -\frac{\pi r j_{d/2-1}(\pi r)}{j_{d/2}(\pi r)} > 0$.*

Lemma 3.11.

$$\Omega((\Delta - \gamma_{\text{res}}) \wedge 1) \cdot \|\lambda\|_2^2 \leq \int_{B^2(R)} \left| \sum_{j=1}^k \lambda_j e^{-2\pi i \langle \mu_j, \omega \rangle} \right|^2 d\psi(\omega) \leq k \|\lambda\|_2^2 \quad (10)$$

where $d\psi(\omega)$ denotes the uniform probability measure over $B^2(R)$ for $R = \frac{\gamma_{\text{res}}}{2\Delta}$.¹

Proof. The upper bound follows by (8). We now show the lower bound. By Theorem 3.4 applied to $d = 2$, for any $\gamma_{\text{res}}/2 < r < \frac{j_{1,1}}{\pi}$ there is a function M which minorizes the indicator function of $B^2(1)$ and has Fourier transform supported in $B^2(r)$. Take $r = \{\Delta R \wedge \frac{\gamma_{\text{res}}/2 + j_{1,1}/\pi}{2}\}$ which satisfies $\gamma_{\text{res}}/2 < r < \frac{j_{1,1}}{\pi}$. This implies that the function $M'(\omega) \triangleq \frac{1}{\pi R^2} \cdot \frac{1}{R} \cdot M(\omega/R)$ minorizes the density $\psi(\omega)$, has Fourier transform supported in $B^2(r) \subseteq B^2(\Delta)$, and satisfies

$$\widehat{M}'[0] = \frac{1}{\pi R^2} \frac{(2/r)^2}{|\mathbb{S}^1|} \cdot \frac{C(2,r)}{1+C(2,r)/2} = \frac{4C(2,r)}{\pi^2 r^3 R^2 \cdot (2+C(2,r))} \geq \frac{r - \gamma_{\text{res}}/2}{R^2} \geq 4r - 2\gamma_{\text{res}}, \quad (11)$$

where in the last step we used that $R < 1/2$. We can lower bound (10) by

$$\begin{aligned} \int \left| \sum_{j=1}^k \lambda_j e^{-2\pi i \langle \mu_j, \omega \rangle} \right|^2 \cdot M'(\omega) d\omega &= \sum_{j,j'=1}^k \lambda_j \lambda_{j'}^\dagger \int e^{-2\pi i \langle \mu_j - \mu_{j'}, \omega \rangle} \cdot M'(\omega) d\omega \\ &= \sum_{j,j'=1}^k \lambda_j \lambda_{j'}^\dagger \widehat{M}'[\mu_j - \mu_{j'}] \geq (4r - 2\gamma_{\text{res}}) \|\lambda\|_2^2, \end{aligned}$$

where the last step follows by (11) and the fact that $\widehat{M}'[\mu_j - \mu_{j'}] = 0$ for all $j \neq j'$. The lemma follows from noting that $4r - 2\gamma_{\text{res}} > \{2\gamma_{\text{res}}(\Delta/c - 1)\} \wedge \left\{ \frac{2j_{1,1}}{\pi} - \gamma_{\text{res}} \right\} \geq O(\Delta - \gamma_{\text{res}} \wedge 1)$. \square

¹In fact, one can improve the upper bound in (10) by using a suitable majorant for the indicator of the ball, but because we are only after polynomial time and sample complexity, this is not needed.

Putting everything together, we have the following guarantee:

Lemma 3.12. *Let ρ be a Δ -separated superposition of k Airy disks. For any $\epsilon_1, \epsilon_2, \delta > 0$, let*

$$m = \Theta\left(\frac{k^2 \log(1/\delta)}{(\Delta - \gamma_{\text{res}}) \wedge 1}\right) \quad \text{and} \quad \eta = O\left(\frac{4\Delta^3 \delta \lambda_{\min}^2}{(\Delta - \gamma_{\text{res}}) k^{5/2} m^{3/2} \kappa(V)^5} \cdot \epsilon_1\right). \quad (12)$$

Without loss of generality suppose $\epsilon_1 < 1/6$. Then the output $(\lambda_1^, \lambda_2^*, \boldsymbol{\mu}_1^*, \boldsymbol{\mu}_2^*)$ of TENSORRESOLVE, given $\epsilon_1, \epsilon_2, \delta$ and access to an η -approximate, m -query OTF oracle \mathcal{O} for ρ , satisfies*

$$\|\boldsymbol{\mu}_i - \boldsymbol{\mu}_{\tau(i)}^*\|_2 \leq \epsilon_1 \quad \text{and} \quad |\lambda_i - \lambda_{\tau(i)}| \leq \epsilon_2$$

for some permutation τ with probability at least $1 - \delta$. Furthermore, the runtime of LEARNAIRY-DISKS is polynomial in k , the number of OTF oracle queries, and the time it takes to make those queries.

Proof. By Lemma 3.7, if we take $m = \Theta\left(\frac{k^2 \log(1/\delta)}{(\Delta - \gamma_{\text{res}}) \wedge 1}\right)$ and $\eta' = O\left(\frac{(c - \gamma_{\text{res}}) \delta \Delta \lambda_{\min}^2}{k^{5/2} m^{3/2} \kappa(V)^5} \cdot \epsilon_1\right)$, then the output \hat{V} of JENNRICH($\tilde{\mathbf{T}}$) satisfies $\|\hat{V} - V\Pi\|_F \leq \epsilon_1$ for some permutation matrix Π . Assume without loss of generality that $\Pi = \text{Id}$. Then we get that for all $j \in [k]$ and $\ell \in [m']$,

$$|\hat{V}_{\ell,j} - V_{\ell,j}| = \left| e^{-2\pi i \langle \hat{\mu}_j - \mu_j, \omega^{(\ell)} \rangle} - 1 \right| \leq \epsilon_1,$$

and because of the elementary inequality $|e^{-2\pi i x} - 1| \geq 2|x|$ for any $|x| \leq 2/3$ and the fact that

$$\langle \hat{\mu}_j - \mu_j, \omega^{(\ell)} \rangle \leq \|\hat{\mu}_j - \mu_j\|_2 \|\omega^{(\ell)}\|_2 \leq 2\mathcal{R} \leq 2/3, \quad (13)$$

we conclude that $|\langle \hat{\mu}_j - \mu_j, \omega^{(\ell)} \rangle| \leq \epsilon_1/2$ for all $j \in [k]$, $\ell \in [m']$. In particular, this holds for all $\ell = m + 1$ and $\ell = m + 2$, so $\|\hat{\mu}_j - \mu_j\|_\infty \leq \epsilon_1$. By dividing ϵ_1 by $\sqrt{2}$ and absorbing constants, we get that the estimates $\{\hat{\mu}_j\}$ for the centers are ϵ_1 -close to the true centers.

To show that the mixing weights are ϵ_2 -close to the true mixing weights, we can apply Lemma 3.8 to conclude that

$$\|\lambda - \hat{\lambda}\|_2 \leq O\left(\frac{\epsilon_1 + \eta'}{k^2 \log(1/\delta) - \epsilon_1}\right) = O\left(\frac{\epsilon_1}{k^2 \log(1/\delta)}\right),$$

so, possibly by modifying ϵ_1 to be $\frac{\epsilon_2}{k^2 \log(1/\delta)}$, we get that the estimates $\{\hat{\lambda}_j\}$ for the mixing weights are ϵ_2 -close to the true mixing weights. \square

Note that we can also amplify the success probability of TENSORRESOLVE by running SELECT from Section 3.2, but we do not belabor this point here.

3.4 Approximating the Optical Transfer Function

In this section, we show that the following algorithm DFT is a valid implementation of an approximate OTF oracle. We begin by showing that when the samples have granularity $\varsigma = 0$, DFT can achieve arbitrarily small error with polynomially many samples.

Lemma 3.13. *For any $0 < \beta < 1$, $\eta > 0$, and frequencies $\omega_1, \dots, \omega_m \in \mathbb{R}^2$, DFT($\{\omega_i\}_{i \in [m]}$) draws $N = O(\log(m/\beta)/\eta^2)$ samples and in time $T = O(N \cdot m)$ outputs numbers u_1, \dots, u_m for which $|u_j - \hat{\rho}[\omega_j]| \leq \eta$.*

Algorithm 6 DFT

- 1: **Input:** Error tolerance $\eta > 0$, sample access to ρ , confidence parameter $\beta > 0$, frequencies $\omega_1, \dots, \omega_m$
 - 2: **Output:** With probability at least $1 - \beta$, numbers u_1, \dots, u_m such that for each $j \in [m]$, $|u_j - \widehat{\rho}[\omega_j]| \leq \eta$
 - 3: $N \leftarrow O(\log(m/\beta)/\eta^2)$.
 - 4: Draw samples $\mathbf{x}_1, \dots, \mathbf{x}_N$ from ρ .
 - 5: For each $j \in [m]$, compute the average $u_j \leftarrow \frac{1}{N} \sum_{i=1}^N \cos(2\pi \cdot \langle \omega_j, \mathbf{x}_i \rangle)$.
 - 6: Output u_1, \dots, u_m .
-

Proof. By a union bound, it suffices to show that for any single $j \in [m]$, $|u_j - \widehat{\rho}[\omega_j]| \leq \eta$ with probability at least $1 - \beta/m$. Note that

$$\mathbb{E}[u_j] = \mathbb{E}_{\mathbf{x} \sim \rho}[\cos(2\pi \cdot \langle \omega_j, \mathbf{x} \rangle)] = \mathbb{E}[\operatorname{Re} \widehat{\rho}[\omega_j]] = \widehat{\rho}[\omega_j],$$

where the last step follows by the fact that $\widehat{\rho}$ is real-valued (by circular symmetry of A). Furthermore, the summands in $\sum_{i=1}^N \cos(2\pi \cdot \langle \omega_j, \mathbf{x}_i \rangle)$ are $[-1, 1]$ -valued, so by Chernoff,

$$\Pr[|u_j - \mathbb{E}[u_j]| > \eta] \leq \exp(-\Omega(N\eta^2)),$$

from which the lemma follows by our choice of N . \square

We now show that for general granularity $\varsigma > 0$, the output of DFT still achieves error $\eta + O(\varsigma)$.

Corollary 3.2. *For any $0 < \beta < 1$, $\eta, \varsigma > 0$, and frequencies $\omega_1, \dots, \omega_m \in \mathbb{R}^2$, if DFT($\{\omega_i\}_{i \in [m]}$) draws $N = O(\log(m/\beta)/\eta^2)$ samples of granularity ς , then in time $T = O(N \cdot m)$ it outputs numbers u_1, \dots, u_m for which $|u_j - \widehat{\rho}[\omega_j]| \leq \eta + O(\varsigma \cdot \|\omega_j\|_2)$.*

Proof. Note that $\cos(\cdot)$ is α -Lipschitz for some $\alpha < 3/4$. This implies that for any $\omega \in \mathbb{R}^2$, the function $\mathbf{x} \mapsto \cos(2\pi \langle \mathbf{x}, \omega \rangle)$ is at most $O(\|\omega\|_2)$ -Lipschitz with respect to ℓ_2 .

Take any collection of 0-granular samples $\mathbf{x}'_1, \dots, \mathbf{x}'_N$ for which the averages u'_1, \dots, u'_m computed by DFT would be η -accurate. If DFT were instead passed ς -granular samples $\mathbf{x}_1, \dots, \mathbf{x}_N$ for which $\|\mathbf{x}'_i - \mathbf{x}_i\|_2 \leq \varsigma$ for each $i \in [N]$, then by triangle inequality, the averages u_1, \dots, u_m computed by DFT with these samples would satisfy $|u_j - u'_j| \leq \eta + O(\varsigma \cdot \|\omega_j\|_2)$ for each $j \in [m]$, as claimed. \square

Finally, with Lemma 3.6 and Lemma 3.13, we can complete the proof of Theorem 3.1.

Proof of Theorem 3.1. By Lemma 3.6, it suffices to produce an η -approximate, m -query OTF oracle for η defined in (6) and $m = O(\log 1/\delta)$. By Corollary 3.2, this can be done using

$$\log(m/\delta)/\eta^2 = \widetilde{O}\left(\log(1/\delta) \cdot \operatorname{poly}(1/\lambda_{\min}, 1/\epsilon_1, 1/\epsilon_2, (4k/\Delta)^{k^2})\right)$$

samples of granularity $\eta/2$ with probability at least $1 - \delta$. Theorem 3.1 then follows by a union bound over the failure probabilities of LEARNIRYDISKS and DFT, and replacing 2δ with δ and absorbing constant factors. Finally, note that the dependence on \mathcal{R} follows by the discussion at the end of Section 3.1. \square

Proof of Theorem 3.2. By Lemma 3.12, it suffices to produce an η -approximate, m -query OTF oracle for η defined in (12) and $m = \Theta\left(\frac{k^2}{(\Delta - \gamma_{\text{res}}) \wedge 1}\right)$. By Corollary 3.2, this can be done with probability 9/10 using

$$\log(10m)/\eta^2 = \widetilde{O}\left(\operatorname{poly}(k, 1/\Delta, 1/\lambda_{\min}, 1/\epsilon_1, 1/\epsilon_2, k, (\Delta - \gamma_{\text{res}}) \wedge 1)\right)$$

samples of granularity $\eta/2$ with probability at least $1 - \delta$. Theorem 3.1 then follows by a union bound over the failure probabilities of TENSORRESOLVECORRECT and DFT. As in the proof of Theorem 3.1, the dependence on \mathcal{R} follows by the discussion at the end of Section 3.1. \square

4 Information Theoretic Lower Bound

In this section we will exhibit two superpositions of Airy disks, both with minimum separation below the diffraction limit, which are close in statistical distance. Let ρ and ρ' respectively have mixing weights $\{\lambda_i\}$ and $\{\lambda'_i\}$, and centers $\{\boldsymbol{\mu}_i\}$ and $\{\boldsymbol{\mu}'_i\}$, where for each i , $\boldsymbol{\mu}_i \triangleq (a_i, 0)$ and $\boldsymbol{\mu}'_i \triangleq (b_i, 0)$ for some $a_i, b_i \in \mathbb{R}$. Concretely,

$$\rho(\mathbf{x}) = \sum_{i=1}^{\lfloor k/2 \rfloor} \lambda_i \cdot A\left(\frac{\|\mathbf{x} - \boldsymbol{\mu}_i\|}{\sigma}\right) \quad \text{and} \quad \rho'(\mathbf{x}) = \sum_{i=1}^{\lfloor k/2 \rfloor} \lambda'_i \cdot A\left(\frac{\|\mathbf{x} - \boldsymbol{\mu}'_i\|}{\sigma}\right)$$

for some $0 < \sigma < 1$. Note that the diffraction limit in this case is $\pi\sigma$.

Theorem 4.1. *There exists a choice of $\{a_i\}$, $\{b_i\}$, $\{\lambda_i\}$, $\{\lambda'_i\}$ such that the minimum separation among centers of ρ and among centers of ρ' is $\Delta = (1 - \epsilon)\pi\sigma$, and $d_{TV}(\rho, \rho') \leq 2^{-\Omega(\epsilon k)}$.*

For convenience, define

$$m \triangleq \frac{2}{(1 - \epsilon)\pi\sigma} \tag{14}$$

so that $\Delta = 2/m$.

A key step will be to bound $\|\rho - \rho'\|_{L^2}$. By Plancherel's theorem, we know that

$$\begin{aligned} \|\rho - \rho'\|_{L^2}^2 &= \|\widehat{\rho} - \widehat{\rho}'\|_{L^2}^2 \\ &= \sigma^2 \int_{\mathbb{R}^2} \widehat{A}[\sigma\omega]^2 \left(\sum_i \lambda_i e^{-2\pi i \langle \boldsymbol{\mu}_i, \omega \rangle} - \sum_i \lambda'_i e^{-2\pi i \langle \boldsymbol{\mu}'_i, \omega \rangle} \right)^2 d\omega \\ &\leq \sigma^2 \int_{B_{1/\pi\sigma}(0)} (1 - \|\pi\sigma\omega\|)^2 \cdot \left(\sum_i \lambda_i e^{-2\pi i \langle \boldsymbol{\mu}_i, \omega \rangle} - \sum_i \lambda'_i e^{-2\pi i \langle \boldsymbol{\mu}'_i, \omega \rangle} \right)^2 d\omega \\ &= \sigma^2 \int_{-\frac{1}{\pi\sigma}}^{\frac{1}{\pi\sigma}} \int_{-\sqrt{\frac{1}{\pi^2\sigma^2} - y^2}}^{\sqrt{\frac{1}{\pi^2\sigma^2} - y^2}} (1 - \pi\sigma\sqrt{x^2 + y^2})^2 \cdot \left(\sum_i \lambda_i e^{-2\pi i a_i x} - \sum_i \lambda'_i e^{-2\pi i b_i x} \right)^2 dx dy, \end{aligned} \tag{15}$$

where the equality follows by the elementary bound

$$\frac{2}{\pi} (\arccos(\pi r) - \pi r \sqrt{1 - \pi^2 r^2}) \leq 1 - \pi r.$$

Without loss of generality suppose k is odd and define

$$c_j = \Delta j/2, \quad j \in \left[-\frac{k-1}{2}, \dots, \frac{k-1}{2} \right]. \tag{16}$$

Lemma 4.1. *There exists a vector $u \in \mathbb{R}^k$ for which $\sum_{j=-(k-1)/2}^{(k-1)/2} u_j e^{-2\pi i c_j x} \leq 2^{-\Omega(\epsilon k)}$ for all $|x| \leq 1/\pi\sigma$. Furthermore, the signs of the entries of u are alternating and*

$$\sum_{j \text{ odd}} |u_j| = \sum_{j \text{ even}} |u_j| = 1. \tag{17}$$

We show this by drawing upon techniques from [Moi15] which were used to show impossibility results for the related problem of learning superpositions of *one-dimensional* Dirac delta functions from their truncated Fourier transforms.

Definition 4.1. *The Fejer kernel is given by*

$$K_\ell(x) = \frac{1}{\ell^2} \sum_{j=-\ell}^{\ell} (\ell - |j|) e(jx) = \frac{1}{\ell^2} \left(\frac{\sin \ell \pi x}{\sin \pi x} \right)^2. \quad (18)$$

We will denote the r -th power of $K_\ell(\cdot)$ by $K_\ell^r(\cdot)$.

Fact 3. K_ℓ is even and periodic with period 1. For $x \in [-1/2, 1/2]$, $K_\ell(x) \leq \frac{1}{4\ell^2 x^2}$.

Proof. That K_ℓ is even and periodic follow from the second definition of K_ℓ in (18). For the bound on K_ℓ , we can use the elementary bounds $\sin \pi x \geq 2x$ for $x \in [0, 1/2]$ and $(\sin \ell \pi x)^2 \leq 1$. \square

Proof of Lemma 4.1. Let $\ell = 4/\epsilon$ and $r = (k-1)/2\ell$. Consider the function

$$H(x) = K_\ell^r(x/m - 1/2).$$

We know that $\widehat{K}_\ell[t] = \frac{1}{\ell^2} \sum_{j=-\ell}^{\ell} (\ell - |j|) \delta(t - j)$, so $\widehat{K}_\ell^r[t] = \sum_{j=-r\ell}^{r\ell} \alpha_j \delta(t - j)$ for nonnegative α_j which sum to 1. We conclude that

$$\widehat{H}[t] = \sum_{j=-(k-1)/2}^{(k-1)/2} h_j e^{-\pi i m t} \delta(mt - j),$$

where $h_j = m\alpha_j$ for $j \neq 0$ and $h_0 = \alpha_0$. We will take

$$u_j \triangleq h_j e^{-\pi i m} \quad \forall j \in \left[-\frac{k-1}{2}, \frac{k-1}{2} \right]$$

where without loss of generality suppose that m defined by (14) is an odd integer so that each u_j is real and alternating in sign as j varies.

By taking the inverse Fourier transform of \widehat{H} , we conclude that

$$H(x) = \sum_{j=-(k-1)/2}^{(k-1)/2} u_j e^{2\pi i j x / m}. \quad (19)$$

To complete our proof, it therefore suffices to show that $H(x) \leq 2^{-\Omega(k)} \|u\|_2$ for all $|x| \leq 1/\pi\sigma$.

But as x ranges across $[-1/\pi\sigma, 1/\pi\sigma]$, $x/m - 1/2$ ranges across $[-1 + \epsilon, -\epsilon]$. By periodicity of K_ℓ , the image of $[-1 + \epsilon, -\epsilon]$ under K_ℓ is no different from that of $[-1/2, -\epsilon] \cup [\epsilon, 1/2]$. We conclude by the bound in Fact 3 that $H(x) = K_\ell^r(x/m - 1/2) \leq \frac{1}{4^{2r}}$ for all $x \in [-1/\pi\sigma, 1/\pi\sigma]$.

The last step is just to scale u so that (17) holds. First note that by substituting $x = 0$ into (19), we have that

$$\sum u_j = H(0) = K_\ell^r(-1/2) = \frac{1}{\ell^{2r}} \sin^{2r}(\ell\pi/2).$$

In particular, if ℓ is even, which we may and shall assume without loss of generality, then $H(0) = 0$. Together with the above observation that the entries of u are indeed alternating in sign, we get the first equality in (17). Finally, note that $\sum |u_j| > 1$ because $\sum \alpha_j = 1$ and $h_j \geq \alpha_j$ for all j . Thus, by multiplying the entries of u by a factor of at most 2, we get the second equality in (17). \square

As the entries $u_{-(k-1)/2}, \dots, u_{(k-1)/2}$ of the vector u constructed in Lemma 4.1 are alternating in sign, and we may without loss of generality suppose that $u_{-(k-1)/2} \geq 0$, we will define

$$\lambda_i = u_{-(k-1)/2+2(i-1)} \quad \forall 1 \leq i \leq \frac{k+1}{2} \quad \text{and} \quad \lambda'_i = -u_{-(k-1)/2+2i-1} \quad \forall 1 \leq i \leq \frac{k-1}{2}$$

for the mixing weights and

$$a_i = c_{-(k-1)/2+2(i-1)} \quad \forall 1 \leq i \leq \frac{k+1}{2} \quad \text{and} \quad b'_i = c_{-(k-1)/2+2i-1} \quad \forall 1 \leq i \leq \frac{k-1}{2},$$

where $\{c_j\}$ are defined by (16), for the first coordinates of the centers $\{\mu_i\} = \{(a_i, 0)\}$ and $\{\mu'_i\} = \{(b_i, 0)\}$. Note that $\{\lambda_i\}$ and $\{\lambda'_i\}$ both consist solely of nonnegative scalars and respectively sum to 1, so ρ, ρ' are valid superpositions of Airy disks. Furthermore, by design,

$$\sum_j u_j e^{-2\pi i c_j x} = \sum_i \lambda_i e^{-2\pi i a_i x} - \sum_i \lambda'_i e^{-2\pi i b_i x},$$

so we may now bound (15) to get

$$\|\rho - \rho'\|_{L^2}^2 \leq 2^{-\Omega(\epsilon k)} \sigma^2 \int_0^{2\pi} \int_0^{\frac{1}{\pi\sigma}} r(1 - \pi\sigma r)^2 dr d\theta \leq 2^{-\Omega(\epsilon k)} \cdot \frac{1}{6\pi}.$$

We are now ready to show that $d_{\text{TV}}(\rho, \rho')$ is small. The following is a generic L^1 bound for functions whose univariate restrictions have bounded L^2 mass, whose derivatives inside some region Ω are bounded, and which decay sufficiently quickly outside of Ω .

Lemma 4.2. *Suppose for an $f \in L^1(\mathbb{R}^2)$, there exists some $T \geq 0$ such that for $\Omega = [-T, T]^2$ the following are satisfied:*

1. For all $y \in [-T, T]$, $\max_{x \in [-T, T]} |f'(x, y)| \leq C$,
2. $\int_{\Omega^c} |f| \leq \eta$,
3. $f(-T, y) \leq \delta$ for all $y \in [-T, T]$.

Then we have that

$$\|f\|_{L^1} \leq (2T)^{5/3} \cdot (3C\|f\|_{L^2}^2 + 2T\delta^3)^{1/3} + \eta.$$

Proof. By the triangle inequality and condition 3, it is enough to verify that

$$\int_{\Omega} |f| \leq (2T)^{5/3} \cdot (3C\|f\|_{L^2}^2 + 2T\delta^3)^{1/3}.$$

Note that for a fixed $y \in [-T, T]$, we have by the fundamental theorem of calculus and conditions 2 and 3 that for any $x \in [-T, T]$,

$$\frac{1}{3}|f(x, y)^3| \leq \frac{1}{3}|f(-T, y)^3| + \left(\int_{-T}^x f(t, y)^2 dt \right) \cdot \max_{t \in [-T, x]} |f'(t, y)| \leq \frac{1}{3}\delta^3 + C \int_{-T}^x f(t, y)^2 dt.$$

Define $g(y) \triangleq \int_{-T}^T f(t, y)^2 dt$ and note that $\int_{-T}^T g(y) dy \leq \|f\|_{L^2}^2$. Then

$$\begin{aligned}
\int_{\Omega} |f| &= \int_{-T}^T \int_{-T}^T |f(x, y)| dx dy \\
&\leq \int_{-T}^T \int_{-T}^T (3C \cdot g(y) + \delta^3)^{1/3} dx dy \\
&= 2T \int_{-T}^T (3C \cdot g(y) + \delta^3)^{1/3} dy \\
&\leq (2T)^2 \left(\int_{-T}^T \frac{1}{2T} (3C \cdot g(y) + \delta^3) dy \right)^{1/3} \\
&= (2T)^{5/3} \left(\int_{-T}^T (3C \cdot g(y) + \delta^3) dy \right)^{1/3} \\
&\leq (2T)^{5/3} \cdot (3C \|f\|_{L^2}^2 + 2T \delta^3)^{1/3},
\end{aligned}$$

where the penultimate inequality follows from the measure-theoretic generalization of Jensen's inequality. \square

We will show that for an appropriate choice of T , the function $f : \mathbb{R}^2 \rightarrow \mathbb{R}$ given by

$$f(\mathbf{x}) \triangleq \rho(\mathbf{x}) - \rho'(\mathbf{x}) = \sum_{i=1}^{(k+1)/2} \lambda_i \cdot A\left(\frac{\|\mathbf{x} - \boldsymbol{\mu}_i\|}{\sigma}\right) - \sum_{i=1}^{(k-1)/2} \lambda'_i \cdot A\left(\frac{\|\mathbf{x} - \boldsymbol{\mu}'_i\|}{\sigma}\right) \quad (20)$$

satisfies the conditions of Lemma 4.2.

For $a, y \in \mathbb{R}$, define $A_{a,y} : \mathbb{R} \rightarrow \mathbb{R}$ by

$$A_{a,y}(x) = A\left(\frac{\sqrt{(x-a)^2 + y^2}}{\sigma}\right).$$

As we will see below, by linearity it will suffice to verify certain properties of $A_{a,y}$.

Lemma 4.3. *For any $y \in \mathbb{R}$, $\max_{x \in \mathbb{R}} |f'(x, y)| = O(1/\sigma)$.*

Proof. By linearity, it suffices to show that for any $a, y \in \mathbb{R}$, $\max_{x \in \mathbb{R}} \left| \frac{\partial A_{a,y}(x)}{\partial x} \right| = O(1/\sigma)$. Of course we may as well assume $a = 0$, in which case by a change of variable in x , we have that

$$\begin{aligned}
\max_{x \in \mathbb{R}} \left| \frac{\partial A_{a,y}(x)}{\partial x} \right| &= \frac{1}{\pi\sigma} \max_x \left| \frac{\partial}{\partial x} \frac{J_1(\sqrt{x^2 + (y/\sigma)^2})^2}{x^2 + (y/\sigma)^2} \right| \\
&= \frac{1}{\pi\sigma} \max_x \left| \frac{2x J_1(\sqrt{x^2 + (y/\sigma)^2}) \cdot J_2(\sqrt{x^2 + (y/\sigma)^2})}{(x^2 + (y/\sigma)^2)^{3/2}} \right| \\
&\leq \frac{1}{\pi\sigma} \max_x \left| \frac{2\sqrt{x^2 + (y/\sigma)^2} J_1(\sqrt{x^2 + (y/\sigma)^2}) \cdot J_2(\sqrt{x^2 + (y/\sigma)^2})}{(x^2 + (y/\sigma)^2)^{3/2}} \right| \\
&= \frac{1}{\pi\sigma} \max_z \left| \frac{2J_1(z)J_2(z)}{z^2} \right| \\
&= \frac{1}{\sigma} \max_z \left| \frac{\partial A(z)}{\partial z} \right| \\
&\leq O(1/\sigma),
\end{aligned}$$

where the final step follows from the fact that the first derivative of A is bounded. \square

Lemma 4.4. For $T > \Delta(k-1)/4$, we have that $f(-T, y) \leq \Omega((T/\sigma)^{-8/3})$ for all y .

Proof. By linearity, it suffices to show that for any $y \in [-T, T]$ and any c_j , the claimed bound holds for $A_{c_j, y}(-T)$. By Theorem 2.1, we know that

$$A_{c_j, y}(-T) \leq \frac{1}{\pi} c_1^2 \cdot |r|^{-8/3},$$

where

$$r \triangleq \frac{(-T - c_j)^2 + y^2}{\sigma} \geq \frac{-T - c_j}{\sigma} > -2T/\sigma,$$

where in the last step we used the fact that $c_j \leq c_{(k-1)/2} \leq \Delta(k-1)/4 < T$. \square

Lemma 4.5. For $T > \Delta(k-1)/2$, we have that $\int_{\Omega^c} |f| \leq O(T^{-2/3} \sigma^{8/3})$, where $\Omega = [-T, T]^2$.

Proof. By linearity and the fact that $\|\mathbf{x} - (c_j, 0)\|_2 \geq T - c_j \geq T/2$ for every $\mathbf{x} \notin \Omega$, it suffices to show that for any c_j , the claimed bound holds for $\int_{B_0(T/2)^c} |A_{c_j, y}(x)| dx dy$. Expressing this as a polar integral, we have

$$\begin{aligned} \int_{B_0(T)^c} |A_{c_j, y}(x)| dx dy &= \int_0^{2\pi} \int_{T/2}^{\infty} r \cdot |A(r/\sigma)| dr d\theta \\ &\leq 2 \cdot \int_{T/2}^{\infty} r \cdot (c_1^2 \cdot (r/\sigma)^{-8/3}) \\ &\leq O(T^{-2/3} \sigma^{8/3}), \end{aligned}$$

as desired. \square

Proof of Theorem 4.1. Take $T = \Theta(\|f\|_{L^2}^{-1/5})$. By (4.2) and Lemmas 4.3, 4.4, and 4.5, we have that for f defined by (20),

$$\begin{aligned} \int_{\mathbb{R}^2} |f| &\leq (2T)^{5/3} \cdot \left(O(1/\sigma) \cdot \|f\|_{L^2}^2 + O(T \cdot (T/\sigma)^{-8}) \right)^{1/3} + O\left(T^{-2/3} \sigma^{8/3}\right) \\ &\leq O\left(\|f\|_{L^2}^{2/15} \sigma^{-1/3}\right) \\ &\leq O(2^{-\Omega(\epsilon k)} \sigma^{-1/3}), \end{aligned}$$

so as soon as $k \geq C \log(1/\sigma)$ for sufficiently large $C > 0$, we have that $d_{\text{TV}}(\rho, \rho') \leq 2^{-\Omega(\epsilon k)}$. \square

Remark 4.1. For the lower bound instance considered in Theorem 4.1, if instead $\Delta \geq (1 + \epsilon)\pi\sigma$, then it is possible to learn the locations of the Airy disks in time polynomial in k . Because we know the line that the centers lie on, we can project in that direction to reduce the problem to a univariate problem, after which we can use the approach of Section 3.2 to deconvolve the distribution by the Airy point spread function and reduce the problem to recovering a spike train from noisy band-limited Fourier measurements. We can then invoke the algorithm of Moitra [Moi15] to learn the spike train in polynomial time as soon as $\Delta \geq (1 + \epsilon)\pi\sigma$. In summary, this together with Theorem 4.1 implies that when the centers are on a line, the Abbe limit marks a sharp phase transition where the sample complexity goes from polynomial to exponential in k as one goes below the Abbe limit.

Remark 4.2. The above construction of convolving many scalings of the Fejer kernel can be traced as far back as to the work of Ingham [Ing34]; indeed, a similar idea is a key step in standard proofs of the Paley-Wiener theorem on the decay of entire functions of exponential type.

5 Conclusion

The question of whether the physics of diffraction imposes fundamental limits on what can be resolved has been a constant source of debate in the optics community since the pioneering work of Abbe, Airy, and Rayleigh in the 1800s. In this work we re-examined this question through the algorithmic lens of learning theory by posing the question as a problem about recovering the parameters of the natural mixture model that arises from first principles of Fraunhofer diffraction. We showed that given the diffraction image of a collection of k point sources of light, the problem of resolving the locations of those point sources is tractable when k is bounded but otherwise exhibits a phase transition in sample complexity above and below the Abbe limit (up to a constant factor of ≈ 1.530). Along the way, we made critical use of an extremal function from the literature on de Branges spaces of entire functions.

Taking a step back, when it comes to modern imaging systems like STED microscopes [HW94], before our work it was not clear if any precise meaning could be ascribed to the diffraction limit they seem to be breaking. Moreover with the advent of modern super-resolution microscopy technologies, the challenge of determining the right criterion by which to assess the resolution of an imaging system remains as pressing as ever. As Demmerle et al. [DWSD15] remark:

“The recent introduction of a range of commercial super-resolution instruments means that resolution has once again become a battleground between different microscope technologies and rival companies.”

The question at the center of this battleground is: *Can we rigorously assess what level of resolution these technologies actually achieve, rather than relying on hand-designed benchmarks?* We believe that our work will be a stepping-stone towards a rigorous theory of resolution limits in more sophisticated optical systems.

Acknowledgments We would like to thank Elchanan Mossel and Tim Roughgarden for helpful feedback on earlier versions of this work.

References

- [Abb73] Ernst Abbe. Beiträge zur theorie des mikroskops und der mikroskopischen wahrnehmung. *Archiv für mikroskopische Anatomie*, 9(1):413–418, 1873.
- [AH97] Carmen O Acuna and Joseph Horowitz. A statistical approach to the resolution of point sources. *Journal of Applied Statistics*, 24(4):421–436, 1997.
- [Air35] George Biddell Airy. On the diffraction of an object-glass with circular aperture. *Transactions of the Cambridge Philosophical Society*, 5:283, 1835.
- [AK01] S. Arora and R. Kannan. Learning mixtures of arbitrary Gaussians. In *Proceedings of the 33rd Symposium on Theory of Computing*, pages 247–257, 2001.
- [AM05] D. Achlioptas and F. McSherry. On spectral learning of mixtures of distributions. In *Proceedings of the Eighteenth Annual Conference on Learning Theory (COLT)*, pages 458–469, 2005.
- [AN72] EA Ash and G Nicholls. Super-resolution aperture scanning microscope. *Nature*, 237(5357):510, 1972.

- [Axe81] Daniel Axelrod. Cell-substrate contacts illuminated by total internal reflection fluorescence. *The Journal of Cell Biology*, 89(1):141–145, 1981.
- [BEH07] Stefan Bretschneider, Christian Eggeling, and Stefan W Hell. Breaking the diffraction barrier in fluorescence microscopy by optical shelving. *Physical Review Letters*, 98(21):218103, 2007.
- [BEZ⁺97] LCEO Brand, C Eggeling, C Zander, KH Drexhage, and CAM Seidel. Single-molecule identification of coumarin-120 by time-resolved fluorescence detection: Comparison of one-and two-photon excitation in solution. *The Journal of Physical Chemistry A*, 101(24):4313–4321, 1997.
- [BPS⁺06] Eric Betzig, George H Patterson, Rachid Sougrat, O Wolf Lindwasser, Scott Olenych, Juan S Bonifacino, Michael W Davidson, Jennifer Lippincott-Schwartz, and Harald F Hess. Imaging intracellular fluorescent proteins at nanometer resolution. *Science*, 313(5793):1642–1645, 2006.
- [BS15] Mikhail Belkin and Kaushik Sinha. Polynomial learning of distribution families. *SIAM Journal on Computing*, 44(4):889–911, 2015.
- [Bux37] A Buxton. Xli. note on optical resolution. *The London, Edinburgh, and Dublin Philosophical Magazine and Journal of Science*, 23(154):440–442, 1937.
- [BV08] S Charles Brubaker and Santosh S Vempala. Isotropic pca and affine-invariant clustering. In *Building Bridges*, pages 241–281. Springer, 2008.
- [BVDDD⁺99] E Bettens, D Van Dyck, AJ Den Dekker, J Sijbers, and A Van den Bos. Model-based two-object resolution from observations having counting statistics. *Ultra-microscopy*, 77(1-2):37–48, 1999.
- [BW13] Max Born and Emil Wolf. *Principles of Optics: Electromagnetic Theory of Propagation, Interference and Diffraction of Light*. Elsevier, 2013.
- [CCLM17] Emanuel Carneiro, Vorrapan Chandee, Friedrich Littmann, and Micah B Milinovich. Hilbert spaces and the pair correlation of zeros of the riemann zeta-function. *Journal für die reine und angewandte Mathematik (Crelles Journal)*, 2017(725):143–182, 2017.
- [CFG13] Emmanuel J Candès and Carlos Fernandez-Granda. Super-resolution from noisy data. *Journal of Fourier Analysis and Applications*, 19(6):1229–1254, 2013.
- [CFG14] Emmanuel J Candès and Carlos Fernandez-Granda. Towards a mathematical theory of super-resolution. *Communications on pure and applied Mathematics*, 67(6):906–956, 2014.
- [CGK17] Jacob Carruth, Felipe Gonçalves, and Michael Kelly. The beurling-selberg box minorant problem. *arXiv preprint arXiv:1702.04579*, 2017.
- [CWO16] Jerry Chao, E Sally Ward, and Raimund J Ober. Fisher information theory for parameter estimation in single molecule microscopy: tutorial. *JOSA A*, 33(7):B36–B57, 2016.

- [Das99] Sanjoy Dasgupta. Learning mixtures of gaussians. In *40th Annual Symposium on Foundations of Computer Science*, pages 634–644. IEEE, 1999.
- [Daw67] William Rutter Dawes. *Catalogue of micrometrical measurements of double stars*. Royal Astronomical Society, 1867.
- [DD96] Arnold J Den Dekker. Model-based optical resolution. In *Quality Measurement: The Indispensable Bridge between Theory and Reality (No Measurements? No Science!) Joint Conference-1996: IEEE Instrumentation and Measurement Technology Conference and IMEKO Tec*, volume 1, pages 441–446. IEEE, 1996.
- [DDVdB97] Arnold Jan Den Dekker and A Van den Bos. Resolution: a survey. *JOSA A*, 14(3):547–557, 1997.
- [DF52] G Toraldo Di Francia. Super-gain antennas and optical resolving power. *Il Nuovo Cimento (1943-1954)*, 9:426–438, 1952.
- [DF55] G Toraldo Di Francia. Resolving power and information. *Josa*, 45(7):497–501, 1955.
- [DKS17] Ilias Diakonikolas, Daniel M Kane, and Alistair Stewart. Statistical query lower bounds for robust estimation of high-dimensional gaussians and gaussian mixtures. In *2017 IEEE 58th Annual Symposium on Foundations of Computer Science (FOCS)*, pages 73–84. IEEE, 2017.
- [DKS18] Ilias Diakonikolas, Daniel M Kane, and Alistair Stewart. List-decodable robust mean estimation and learning mixtures of spherical gaussians. In *Proceedings of the 50th Annual ACM SIGACT Symposium on Theory of Computing*, pages 1047–1060, 2018.
- [Don92] David L Donoho. Superresolution via sparsity constraints. *SIAM journal on mathematical analysis*, 23(5):1309–1331, 1992.
- [DS89] David L Donoho and Philip B Stark. Uncertainty principles and signal recovery. *SIAM Journal on Applied Mathematics*, 49(3):906–931, 1989.
- [DS00] S. Dasgupta and L. Schulman. A two-round variant of EM for Gaussian mixtures. In *Proceedings of the 16th Conference on Uncertainty in Artificial Intelligence*, pages 143–151, 2000.
- [DWSD15] Justin Demmerle, Eva Wegel, Lothar Schermelleh, and Ian M Dobbie. Assessing resolution in super-resolution imaging. *Methods*, 88:3–10, 2015.
- [DZM⁺14] Hendrik Deschout, Francesca Cella Zanicchi, Michael Mlodzianoski, Alberto Diaspro, Joerg Bewersdorf, Samuel T Hess, and Kevin Braeckmans. Precisely and accurately localizing single emitters in fluorescence microscopy. *Nature Methods*, 11(3):253, 2014.
- [EKPR18] Martin Ehler, Stefan Kunis, Thomas Peter, and Christian Richter. A randomized multivariate matrix pencil method for superresolution microscopy. *arXiv preprint arXiv:1805.02485*, 2018.

- [Fal67] Oscar Falconi. Limits to which double lines, double stars, and disks can be resolved and measured. *JOSA*, 57(8):987–993, 1967.
- [Far66] Edward J Farrell. Information content of photoelectric star images. *JOSA*, 56(5):578–587, 1966.
- [FB12] Eric D Feigelson and G Jogesh Babu. *Modern Statistical Methods for Astronomy: with R Applications*. Cambridge University Press, 2012.
- [FG13] Carlos Fernandez-Granda. Support detection in super-resolution. *arXiv preprint arXiv:1302.3921*, 2013.
- [FG16] Carlos Fernandez-Granda. Super-resolution of point sources via convex programming. *Information and Inference: A Journal of the IMA*, 5(3):251–303, 2016.
- [FLS11] Richard P Feynman, Robert B Leighton, and Matthew Sands. *The Feynman lectures on physics, Vol. I: The new millennium edition: mainly mechanics, radiation, and heat*, volume 1. Basic books, 2011.
- [Fow89] Grant R Fowles. *Introduction to Modern Optics*. Courier Corporation, 1989.
- [GGI⁺02] Anna C Gilbert, Sudipto Guha, Piotr Indyk, Shanmugavelayutham Muthukrishnan, and Martin Strauss. Near-optimal sparse fourier representations via sampling. In *Proceedings of the thirty-fourth annual ACM symposium on Theory of computing*, pages 152–161, 2002.
- [GHK15] Rong Ge, Qingqing Huang, and Sham M Kakade. Learning mixtures of gaussians in high dimensions. In *Proceedings of the forty-seventh annual ACM symposium on Theory of computing*, pages 761–770, 2015.
- [GIIS14] Anna C Gilbert, Piotr Indyk, Mark Iwen, and Ludwig Schmidt. Recent developments in the sparse fourier transform: A compressed fourier transform for big data. *IEEE Signal Processing Magazine*, 31(5):91–100, 2014.
- [GMS05] Anna C Gilbert, Shan Muthukrishnan, and Martin Strauss. Improved time bounds for near-optimal sparse fourier representations. In *Wavelets XI*, volume 5914, page 59141A. International Society for Optics and Photonics, 2005.
- [Gon18] Felipe Gonçalves. A note on band-limited minorants of an euclidean ball. *Proceedings of the American Mathematical Society*, 146(5):2063–2068, 2018.
- [Goo05] Joseph W Goodman. *Introduction to Fourier Optics*. Roberts and Company Publishers, 2005.
- [Goo15] Joseph W Goodman. *Statistical optics*. John Wiley & Sons, 2015.
- [Gus99] Mats GL Gustafsson. Extended resolution fluorescence microscopy. *Current Opinion in Structural Biology*, 9(5):627–628, 1999.
- [Har64] James L Harris. Resolving power and decision theory. *JOSA*, 54(5):606–611, 1964.

- [HBZ10] Bo Huang, Hazen Babcock, and Xiaowei Zhuang. Breaking the diffraction barrier: super-resolution imaging of cells. *Cell*, 143(7):1047–1058, 2010.
- [Hec15] Eugene Hecht. *Optics*. Pearson, 2015.
- [Hel64] C Helstrom. The detection and resolution of optical signals. *IEEE Transactions on Information Theory*, 10(4):275–287, 1964.
- [Hel69] Carl W Helstrom. Detection and resolution of incoherent objects by a background-limited optical system. *JOSA*, 59(2):164–175, 1969.
- [Hel70] Carl W Helstrom. Resolvability of objects from the standpoint of statistical parameter estimation. *JOSA*, 60(5):659–666, 1970.
- [Hel04] Stefan W Hell. Strategy for far-field optical imaging and writing without diffraction limit. *Physics Letters A*, 326(1-2):140–145, 2004.
- [Hel07] Stefan W Hell. Far-field optical nanoscopy. *Science*, 316(5828):1153–1158, 2007.
- [Hel09] Stefan W Hell. Microscopy and its focal switch. *Nature Methods*, 6(1):24, 2009.
- [HG09] Rainer Heintzmann and Mats GL Gustafsson. Subdiffraction resolution in continuous samples. *Nature Photonics*, 3(7):362, 2009.
- [HGM06] Samuel T Hess, Thanu PK Girirajan, and Michael D Mason. Ultra-high resolution imaging by fluorescence photoactivation localization microscopy. *Biophysical Journal*, 91(11):4258–4272, 2006.
- [HHP⁺16] Roarke Horstmeyer, Rainer Heintzmann, Gabriel Popescu, Laura Waller, and Changhuei Yang. Standardizing the resolution claims for coherent microscopy. *Nature Photonics*, 10(2):68, 2016.
- [HIKP12] Haitham Hassanieh, Piotr Indyk, Dina Katabi, and Eric Price. Nearly optimal sparse fourier transform. In *Proceedings of the forty-fourth annual ACM symposium on Theory of computing*, pages 563–578, 2012.
- [HK95] Stefan W Hell and Matthias Kroug. Ground-state-depletion fluorescence microscopy: A concept for breaking the diffraction resolution limit. *Applied Physics B*, 60(5):495–497, 1995.
- [HK13] Daniel Hsu and Sham M Kakade. Learning mixtures of spherical gaussians: moment methods and spectral decompositions. In *Proceedings of the 4th conference on Innovations in Theoretical Computer Science*, pages 11–20, 2013.
- [HK15] Qingqing Huang and Sham M Kakade. Super-resolution off the grid. In *Advances in Neural Information Processing Systems*, pages 2665–2673, 2015.
- [HL18] Samuel B Hopkins and Jerry Li. Mixture models, robustness, and sum of squares proofs. In *Proceedings of the 50th Annual ACM SIGACT Symposium on Theory of Computing*, pages 1021–1034, 2018.
- [Hou27] William V Houston. A compound interferometer for fine structure work. *Physical Review*, 29(3):478, 1927.

- [HP15] Moritz Hardt and Eric Price. Tight bounds for learning a mixture of two gaussians. In *Proceedings of the 47th Annual ACM Symposium on Theory of Computing*, pages 753–760, 2015.
- [HS92] Stefan Hell and Ernst HK Stelzer. Properties of a 4pi confocal fluorescence microscope. *JOSA A*, 9(12):2159–2166, 1992.
- [HSLC94] Stefan W Hell, Ernst HK Stelzer, Steffen Lindek, and Christoph Cremer. Confocal microscopy with an increased detection aperture: type-b 4pi confocal microscopy. *Optics Letters*, 19(3):222–224, 1994.
- [HV⁺96] Jeffrey J Holt, Jeffrey D Vaaler, et al. The beurling-selberg extremal functions for a ball in euclidean space. *Duke Mathematical Journal*, 83(1):203–248, 1996.
- [HW94] Stefan W Hell and Jan Wichmann. Breaking the diffraction resolution limit by stimulated emission: stimulated-emission-depletion fluorescence microscopy. *Optics Letters*, 19(11):780–782, 1994.
- [IKP14] Piotr Indyk, Michael Kapralov, and Eric Price. (nearly) sample-optimal sparse fourier transform. In *Proceedings of the twenty-fifth annual ACM-SIAM symposium on Discrete algorithms*, pages 480–499. SIAM, 2014.
- [Ing34] AE Ingham. A note on fourier transforms. *Journal of the London Mathematical Society*, 1(1):29–32, 1934.
- [JSZB08] Na Ji, Hari Shroff, Haining Zhong, and Eric Betzig. Advances in the speed and resolution of light microscopy. *Current opinion in neurobiology*, 18(6):605–616, 2008.
- [JW37] Francis A Jenkins and Harvey E White. *Fundamentals of optics*. Tata McGraw-Hill Education, 1937.
- [Kap16] Michael Kapralov. Sparse fourier transform in any constant dimension with nearly-optimal sample complexity in sublinear time. In *Proceedings of the forty-eighth annual ACM symposium on Theory of Computing*, pages 264–277, 2016.
- [Kea98] Michael Kearns. Efficient noise-tolerant learning from statistical queries. *Journal of the ACM (JACM)*, 45(6):983–1006, 1998.
- [Ken08] Ian R Kenyon. *The light fantastic: a modern introduction to classical and quantum optics*. Oxford University Press, USA, 2008.
- [KH99] Thomas A Klar and Stefan W Hell. Subdiffraction resolution in far-field fluorescence microscopy. *Optics Letters*, 24(14):954–956, 1999.
- [KJH95] Janos Kirz, Chris Jacobsen, and Malcolm Howells. Soft x-ray microscopes and their biological applications. *Quarterly reviews of biophysics*, 28(1):33–130, 1995.
- [KMV10] A. T. Kalai, A. Moitra, and G. Valiant. Efficiently learning mixtures of two Gaussians. In *STOC*, pages 553–562, 2010.
- [KPRvdO16] Stefan Kunis, Thomas Peter, Tim Römer, and Ulrich von der Ohe. A multivariate generalization of prony’s method. *Linear Algebra and its Applications*, 490:31–47, 2016.

- [KS17] Pravesh K Kothari and David Steurer. Outlier-robust moment-estimation via sum-of-squares. *arXiv preprint arXiv:1711.11581*, 2017.
- [Lan00] LJ Landau. Bessel functions: monotonicity and bounds. *Journal of the London Mathematical Society*, 61(1):197–215, 2000.
- [Lau12] Marcel A Lauterbach. Finding, defining and breaking the diffraction barrier in microscopy—a historical perspective. *Optical Nanoscopy*, 1(1):8, 2012.
- [Lia15] Wenjing Liao. Music for multidimensional spectral estimation: stability and super-resolution. *IEEE Transactions on Signal Processing*, 63(23):6395–6406, 2015.
- [LSM09] Jennifer Lippincott-Schwartz and Suliana Manley. Putting super-resolution fluorescence microscopy to work. *Nature Methods*, 6(ARTICLE):21–23, 2009.
- [Luc92a] Leon B Lucy. Resolution limits for deconvolved images. *The Astronomical Journal*, 104:1260–1265, 1992.
- [Luc92b] Leon B Lucy. Statistical limits to super resolution. *Astronomy and Astrophysics*, 261:706, 1992.
- [Man59] Leonard Mandel. Fluctuations of photon beams: the distribution of the photoelectrons. *Proceedings of the Physical Society*, 74(3):233, 1959.
- [MC16] Veniamin I Morgenshtern and Emmanuel J Candes. Super-resolution of positive sources: The discrete setup. *SIAM Journal on Imaging Sciences*, 9(1):412–444, 2016.
- [MCSF10] Kim I Mortensen, L Stirling Churchman, James A Spudich, and Henrik Flyvbjerg. Optimized localization analysis for single-molecule tracking and super-resolution microscopy. *Nature Methods*, 7(5):377, 2010.
- [Min61] M Minsky. Microscopy apparatus us patent 3013467. *USP Office, Ed. US*, 1961.
- [Moi15] Ankur Moitra. Super-resolution, extremal functions and the condition number of vandermonde matrices. In *Proceedings of the 47th Annual ACM Symposium on Theory of Computing*, pages 821–830. ACM, 2015.
- [MV10] Ankur Moitra and Gregory Valiant. Settling the polynomial learnability of mixtures of gaussians. In *2010 IEEE 51st Annual Symposium on Foundations of Computer Science*, pages 93–102. IEEE, 2010.
- [MW17] AA Maznev and OB Wright. Upholding the diffraction limit in the focusing of light and sound. *Wave Motion*, 68:182–189, 2017.
- [PDL84] Dieter W Pohl, Winfried Denk, and Mark Lanz. Optical stethoscopy: Image recording with resolution $\lambda/20$. *Applied Physics Letters*, 44(7):651–653, 1984.
- [Ray79] Lord Rayleigh. Investigations in optics, with special reference to the spectroscope. *The London, Edinburgh, and Dublin Philosophical Magazine and Journal of Science*, 8(49):261–274, 1879.

- [RBZ06] Michael J Rust, Mark Bates, and Xiaowei Zhuang. Sub-diffraction-limit imaging by stochastic optical reconstruction microscopy (storm). *Nature Methods*, 3(10):793, 2006.
- [RCK41] BP Ramsay, EL Cleveland, and OT Koppius. Criteria and the intensity-epoch slope. *JOSA*, 31(1):26–33, 1941.
- [Ric07] James H Rice. Beyond the diffraction limit: far-field fluorescence imaging with ultrahigh resolution. *Molecular BioSystems*, 3(11):781–793, 2007.
- [Ron61] Vasco Ronchi. Resolving power of calculated and detected images. *JOSA*, 51(4):458.1–460, 1961.
- [Rus34] Ernst Ruska. Über fortschritte im bau und in der leistung des magnetischen elektronenmikroskops. *Zeitschrift für Physik A Hadrons and Nuclei*, 87(9):580–602, 1934.
- [RV17] Oded Regev and Aravindan Vijayaraghavan. On learning mixtures of well-separated gaussians. In *2017 IEEE 58th Annual Symposium on Foundations of Computer Science (FOCS)*, pages 85–96. IEEE, 2017.
- [RWO06] Sripad Ram, E Sally Ward, and Raimund J Ober. Beyond rayleigh’s criterion: a resolution measure with application to single-molecule microscopy. *Proceedings of the National Academy of Sciences*, 103(12):4457–4462, 2006.
- [Sch04] Arthur Schuster. *An introduction to the theory of optics*. E. Arnold, 1904.
- [She17] Colin JR Sheppard. Resolution and super-resolution. *Microscopy research and technique*, 80(6):590–598, 2017.
- [SM04] Morteza Shahram and Peyman Milanfar. Imaging below the diffraction limit: a statistical analysis. *IEEE Transactions on image processing*, 13(5):677–689, 2004.
- [SM06] Morteza Shahram and Peyman Milanfar. Statistical and information-theoretic analysis of resolution in imaging. *IEEE Transactions on information Theory*, 52(8):3411–3437, 2006.
- [Spa16] Carroll Mason Sparrow. On spectroscopic resolving power. *The Astrophysical Journal*, 44:76, 1916.
- [SS14] Alex Small and Shane Stahlheber. Fluorophore localization algorithms for super-resolution microscopy. *Nature Methods*, 11(3):267, 2014.
- [Syn28] EdwardH Synge. Xxxviii. a suggested method for extending microscopic resolution into the ultra-microscopic region. *The London, Edinburgh, and Dublin Philosophical Magazine and Journal of Science*, 6(35):356–362, 1928.
- [TBSR13] Gongguo Tang, Badri Narayan Bhaskar, Parikshit Shah, and Benjamin Recht. Compressed sensing off the grid. *IEEE transactions on information theory*, 59(11):7465–7490, 2013.

- [TD79] Ming-Jer Tsai and Keh-Ping Dunn. Performance limitations on parameter estimation of closely spaced optical targets using shot-noise detector model. Technical report, MIT Lexington Lincoln Lab, 1979.
- [Tem81] Paul A Temple. Total internal reflection microscopy: a surface inspection technique. *Applied Optics*, 20(15):2656–2664, 1981.
- [Tho69] Brian J Thompson. Iv image formation with partially coherent light. In *Progress in optics*, volume 7, pages 169–230. Elsevier, 1969.
- [Tsa18] Mankei Tsang. Conservative classical and quantum resolution limits for incoherent imaging. *Journal of Modern Optics*, 65(11):1385–1391, 2018.
- [Tsa19] Mankei Tsang. Resolving starlight: a quantum perspective. *arXiv preprint arXiv:1906.02064*, 2019.
- [Vaa85] Jeffrey D Vaaler. Some extremal functions in fourier analysis. *Bulletin of the American Mathematical Society*, 12(2):183–216, 1985.
- [VAdDVDVDB02] S Van Aert, AJ den Dekker, D Van Dyck, and A Van Den Bos. High-resolution electron microscopy and electron tomography: resolution versus precision. *Journal of Structural Biology*, 138(1-2):21–33, 2002.
- [VDB01] Adriaan Van Den Bos. Resolution in model-based measurement. In *IMTC 2001. Proceedings of the 18th IEEE Instrumentation and Measurement Technology Conference. Rediscovering Measurement in the Age of Informatics (Cat. No. 01CH 37188)*, volume 1, pages 295–302. IEEE, 2001.
- [VdBDD01] A Van den Bos and AJ Den Dekker. Resolution reconsidered—conventional approaches and an alternative. In *Advances in imaging and electron physics*, volume 117, pages 241–360. Elsevier, 2001.
- [vDSM17] Alex von Diezmann, Yoav Shechtman, and WE Moerner. Three-dimensional localization of single molecules for super-resolution imaging and single-particle tracking. *Chemical reviews*, 117(11):7244–7275, 2017.
- [VW02] S. Vempala and G. Wang. A spectral algorithm for learning mixtures of distributions. In *Proceedings of the 43rd Annual Symposium on Foundations of Computer Science*, pages 113–122, 2002.
- [Wil50] W Ewart Williams. *Applications of interferometry*. Methuen, London, UK, 1950.
- [WS15] Siegfried Weisenburger and Vahid Sandoghdar. Light microscopy: an ongoing contemporary revolution. *Contemporary Physics*, 56(2):123–143, 2015.
- [WSS01] Wes Wallace, Lutz H Schaefer, and Jason R Swedlow. A workingperson’s guide to deconvolution in light microscopy. *Biotechniques*, 31(5):1076–1097, 2001.
- [Zmu03] Jonas Zmuidzinas. Cramer–rao sensitivity limits for astronomical instruments: implications for interferometer design. *JOSA A*, 20(2):218–233, 2003.

A Related Work In the Sciences

In this section, we survey previous approaches to understanding diffraction limits in the optics literature, as well as recent practical works on the need and methodologies to rigorously assess claims of achieving super-resolution.

A.1 Previous Approaches in Optics

In this section we will survey the many previous attempts to rigorously understand diffraction limits in the optics literature. There, the focus has been squarely on the semiclassical detection model (SDM). After describing this line of work, we explain the ways in which it falls short.

The SDM was originally proposed by [Man59] and has been the *de facto* generative model in essentially all subsequent works on the statistical foundations of resolution. We note that there are some minor differences in the definition of our model and that of the SDM, which we will discuss formally in Appendix B.3.

Arguably the first significant work to study the SDM was that of Helstrom [Hel64], who considered it from the perspective of parameter estimation and hypothesis testing, initiating the study of the following two problems which remarkably have almost exclusively occupied this line of work. For normalized point spread function $A(\cdot)$ and separation parameter d , define

$$\rho_0(\mathbf{x}) = A(\mathbf{x}), \quad \rho_1(\mathbf{x}) = \frac{1}{2} \cdot A(\mathbf{x} - \boldsymbol{\mu}) + \frac{1}{2} \cdot A(\mathbf{x} + \boldsymbol{\mu}), \quad \boldsymbol{\mu} = \begin{cases} d/2 & D = 1 \\ (0, d/2) & D = 2. \end{cases} \quad (21)$$

Problem 1 (Parameter Estimation). *Given samples from ρ_1 , estimate d .*

Problem 2 (Hypothesis Testing). *Suppose we know the parameter d , and we know that either $\rho = \rho_0$ or $\rho = \rho_1$. Given samples from ρ , decide whether $\rho = \rho_0$ or $\rho = \rho_1$.*

For Problem 1, Helstrom [Hel64, Hel69, Hel70] studied the maximum likelihood estimator and computed Cramer-Rao lower bounds for a host of point-spread functions including the Airy PSF, both for the SDM and for progressively more physically sophisticated (though less practically relevant) models. The conceptual insights and problem formulation of [Hel64] were refined, or often rediscovered, numerous times [TD79, BVDDD⁺99, VaDdVDVDB02, SM04, SM06, RWO06, Far66, CWO16], and the primary thrust of this line of work has been centered on Cramer-Rao-style calculations for assorted point-spread functions and, to a lesser extent, analysis of the optimization landscape of the log-likelihood from the perspective of singularity theory [VDB01, VdBDD01, BVDDD⁺99, DD96].

For Problem 2, Helstrom [Hel64] computed the reliability of the likelihood ratio test for various PSFs, under a CLT approximation to the log-likelihood ratio. Similar calculations for the log-likelihood ratio for other PSFs followed in [Har64, AH97, SM04, SM06, Far66].

We emphasize that, with the exception of [SM04, SM06], all works giving rigorous guarantees have made the assumption implicit in (21) that the two point sources defining ρ_1 are located at *known* points $\boldsymbol{\mu}$ and $-\boldsymbol{\mu}$ centered about the origin. [SM04, SM06] study Problems 1 and 2 when the locations of the point sources are unknown and study the (locally optimal) generalized likelihood ratio test.

With regards to applications, Problems 1 and 2 have gained popularity in optical astronomy [Fal67, Zmu03, FB12, Luc92a, Luc92b] as well as fluorescence microscopy [MCSF10, SS14, DZM⁺14, vDSM17]. Cramer-Rao bounds as a “modern” proxy for assessing the limits of imaging systems have gained such popularity with practitioners that a number of review articles and surveys on the

topic have appeared in the recent single-molecule microscopy literature [SS14, DZM⁺14, CWO16], most of which focus on the related parameter estimation problem of *localization*, that is, estimating the location of a *single* test object given its noisy image.

One other interesting line of work has focused on the generalizations of Problems 1 and 2 to the quantum setting. Elaborating on this literature would take us too far afield, so we mention only the comprehensive recent survey [Tsa19] and the references therein.

A.2 Comparison with Our Approach

Most crucially, all works on the SDM focus exclusively on *two*-point resolution. In the context of hypothesis testing, as we note above, these works even assume the two points lie on the x -axis at the same *known* distance $d/2$ from the origin, with the exception of [SM04, SM06]. That such a strong assumption is made and such focus is placed on $k = 2$ is evidently not just for aesthetics. From the standpoint of hypothesis testing, as noted in [SM04, SM06], any deviation from this idealized model would induce a composite hypothesis testing problem, for which the (generalized) likelihood ratio test has no global optimality guarantees. In the context of parameter estimation, because of the focus on $k = 2$, the conclusion in the literature has repeatedly been that the classical resolution criteria (Abbe, Rayleigh, etc.) are not meaningful in a statistical sense, and that the only true limitation comes from the number of samples. We view this as one of the primary reasons that a result like Theorem 1.2 has gone overlooked for so long.

Another drawback of the literature is that because of the focus on Cramer-Rao bounds, which only provide guarantees for the maximum likelihood estimate in the infinite-sample limit, none of these works actually give non-asymptotic algorithmic guarantees. Additionally, Cramer-Rao bounds only apply to unbiased estimators, and to the best of our knowledge, the only paper that addresses biased estimators is [Tsa18], which only derives Bayesian Cramer-Rao bounds for the already well-studied setting of a mixture of two Gaussians. From a technical standpoint, another disadvantage of existing works is that they work either with the Gaussian point-spread function or invoke Taylor approximations of the Airy point-spread function. And because the log-likelihood here is analytically cumbersome, it is common to invoke a central limit theorem-style approximation.

One last shortcoming arises from the definition of the SDM itself (see Definition B.1): it models photon detection as a Poisson process when in reality this need not be the case. As Goodman (Chapter 9.2 of [Goo15]) notes, “in most problems of real interest, however, the light wave incident on the photosurface has stochastic attributes . . . For this reason, it is necessary to regard the Poisson distribution as a *conditional* probability distribution . . . the statistics are in general *not* Poisson when the classical intensity has random fluctuations of its own.” The increased generality of not assuming Poissonianity allows our model to smoothly handle such stochastic fluctuations.

A.3 Super-Resolution and the Practical Need to Understand Diffraction Limits

In the past half century, a host of techniques of increasing sophistication have been developed to shift or fundamentally surpass the diffraction limit. As these techniques change the underlying physical setup of the imaging system, they are not relevant to the theoretical setting we consider, though we believe that placing the classical setting of Fraunhofer diffraction on a rigorous statistical footing can pave the way towards better understanding notions of resolution in these modern techniques. Here we very briefly describe some these techniques, deferring to the comprehensive overviews on the matter found in [HG09, Hel07, Hel09, HBZ10, JSZB08, Lau12, LSM09, MW17, Ric07, WS15]. The earliest attempts at going below the diffraction limit involved modifying the aperture, e.g. via *apodization* as pioneered by Toraldo di Francia [DF52]. Among even more elementary approaches,

an annular aperture can be used to distinguish a pair of points sources slightly better than a circular one, a fact that [MW17] notes was known even to Rayleigh. Other approaches for circumventing the diffraction limit include near-field optics [AN72, PDL84, Syn28], TIRF [Axe81, Tem81], confocal microscopy [Min61], two-lens techniques [HS92, HSLC94], structured illumination [Gus99], UV/X-ray/electron microscopy [BEZ⁺97, KJH95, Rus34].

Betzig, Hell, and Moerner were awarded the 2014 Nobel Prize in Chemistry for their pioneering work on super-resolution microscopy, which now includes technologies such as STED [HW94, KH99], RESOLFT [HK95, Hel04, BEH07], PALM [BPS⁺06], STORM [RBZ06], and FPALM [HGM06]. These fundamentally break the diffraction limit by leveraging the ability to switch fluorescent markers between a bright and a dark state via photophysical effects like stimulated emission and ground-state depletion. In light of such advancements, rigorously characterizing the resolving power of imaging systems remains a challenge of practical as much as theoretical interest. [DWSD15] revisited what resolution means given these new technologies and proposed approaches for comparing resolution between different super-resolution methods. [HHP⁺16] pushed back on some claims of super-resolution in nonfluorescent microscopy, advocating for the Siemens star as an imaging benchmark and for the adoption of certain standards when documenting such claims. Sheppard [She17] was similarly motivated to clarify such claims and calculates the images of various test object geometries and suggests “these results can be used as a reference ... to determine if super-resolution has indeed been attained.”

B Physical Basis for Our Model

In this paper we focus on the idealized setting of Fraunhofer diffraction of incoherent illumination by a circular aperture, originally studied in the pioneering work of Airy [Air35]. In this section, we first give a brief overview of this setting in Appendix B.1, deferring the details to any of a number of excellent expository texts on the subject [Ken08, Hec15, Goo05, Goo15, JW37, Fow89]. Then in Appendix B.2, we demonstrate how our probabilistic model arises naturally from the preceding setup. Finally, in Appendix B.4, we catalogue the various resolution criteria that have appeared in the literature and instantiate them in our framework.

B.1 A Review of Fraunhofer Diffraction

Consider a scenario in which plane waves of monochromatic, incoherent light emanate from a far-away point source in the image plane, pass through a circular aperture, and form a diffraction pattern on a far-away observation plane. This is the standard setting of *Fraunhofer diffraction*. As depicted in Figure 1, the far-field assumption on the observation plane is captured in practice by placing a lens behind the aperture and placing the observation plane at the focal plane of the lens.

Under the Huygens-Fresnel-Kirchhoff theory, the aperture induces a diffraction pattern, a so-called *Airy disk*, on the observation plane because the secondary spherical wavelets emanating from different points of the aperture are off by phase factors. Concretely, suppose the plane waves are parallel to the optical axis, and take a point P on the observation plane at angular distance θ from the optical axis, and a point \mathbf{u} on the circular aperture A , say of radius r . Letting \mathbf{v} be the unit vector from the center of the aperture to P , we see that the propagation path of the wavelet from the center of the aperture to P and that of the wavelet from \mathbf{u} to P differ in length by $\langle \mathbf{u}, \mathbf{v} \rangle$, corresponding to a phase delay of $\frac{2\pi}{\lambda} \langle \mathbf{u}, \mathbf{v} \rangle$ where λ is the wavelength of light. So by integrating over the contributions to the amplitude of the electric field at P by the points \mathbf{u} in A , we conclude

that the amplitude at P is

$$E = E_0 \int_A e^{2\pi i \cdot \langle \mathbf{u}, \mathbf{v} \rangle / \lambda} d\mathbf{u},$$

where E_0 is, up to phase factors, a constant capturing the contribution to the field per unit area of the aperture. In other words, the amplitude at P is proportional to the 2D Fourier transform of the pupil function $F(\mathbf{u}) = \mathbb{1}[\mathbf{u} \in A]$ at frequency \mathbf{v}/λ . This can be computed explicitly as

$$E = 2\pi r^2 E_0 \cdot \frac{J_1(\kappa r \sin \theta)}{\kappa r \sin \theta},$$

where $\kappa \triangleq \frac{2\pi}{\lambda}$ is the wavenumber of the light. In particular, the intensity $I(\theta)$ of the diffraction pattern at P is the squared modulus of E . We conclude that

$$I(\theta) = I(0) \cdot \left(\frac{2J_1(\kappa r \sin \theta)}{\kappa r \sin \theta} \right)^2, \quad (22)$$

where $J_1(\cdot)$ is the Bessel function of the first kind. We will typically regard $I(\cdot)$ as a function $\mathbb{R}^2 \rightarrow \mathbb{R}_{\geq 0}$ which takes in a point $(x, y) \in \mathbb{R}^2$ and outputs $I(\theta)$, where θ is the angular distance between (x, y) and the optical axis. The function $I(x, y)$ is the so-called *Airy point spread function*.

Remark B.1. *In general, if the plane waves of the point source travel at an angle ψ to the optical axis, they will be focused not at the focal point but at some other point on the observation plane at an angular distance of ψ with respect to the optical axis. In this case the resulting Airy point spread function will be shifted to be centered at that point.*

B.2 Photon Statistics and Our Model

First suppose there is a single point source of light. In a sense which can be made rigorous via Feynman's path integral formalism (see e.g. Section 4.11 of [Hec15]), the intensity $I(x, y)$ of the diffraction pattern at a point (x, y) on the observation plane is proportional to the (infinitesimal) probability of detecting a photon at P . That is, the point spread function $I(x, y)$ can be identified with a probability density

$$\rho(x, y) \triangleq \frac{1}{Z} \cdot I(x, y), \quad \text{where } Z \triangleq \int_{\mathbb{R}^2} I(x, y) dx dy$$

over the two-dimensional observation plane. Concretely, for any measurable subset S of the observation plane, if one were to count photons arriving over time and compute the fraction that land inside the region S , this fraction would tend towards $\int_S \rho(x, y) dx dy$.

In the presence of k *incoherent* point sources of light, the absence of interference means that the contributions from each point source to the intensities of the resulting diffraction pattern simply add. In other words, if $I_1(\cdot), \dots, I_k(\cdot)$ are the corresponding point spread functions, which by Remark B.1 are merely shifted versions of (22), the resulting probability density ρ over the observation plane is simply proportional to $\sum_{i=1}^k I_i(\cdot)$.

For every $i \in [k]$, let $Z_i \triangleq \int_{\mathbb{R}^2} I_i(x, y) dx dy$ be the normalizing constant for the i -th density $\rho_i(\cdot) \triangleq \frac{1}{Z_i} I_i(\cdot)$. Let $\lambda_i \triangleq \frac{Z_i}{\sum_{j=1}^m Z_j}$. Then we see that

$$\rho(x, y) = \sum_{i=1}^m \lambda_i \cdot \rho_i(x, y).$$

In the jargon of statistics, this is an example of a *mixture model*, i.e. a convex combination of structured distributions, and one can think of sampling from ρ by first sampling an index $i \in [m]$ with probability λ_i and then sampling a point (x, y) in the observation plane according to the probability density associated to the i -th point source. This brings us to the generative model that we study in this work, the definition of which we restate here for the reader's convenience.

Definition 2.1. [*Superpositions of Airy Disks*] A superposition of k Airy disks ρ is a distribution over \mathbb{R}^2 specified by relative intensities $\lambda_1, \dots, \lambda_k \geq 0$ summing to 1, centers $\boldsymbol{\mu}_1, \dots, \boldsymbol{\mu}_k \in \mathbb{R}^2$, and an a priori known “spread parameter” $\sigma > 0$. Its density is given by

$$\rho(\mathbf{x}) = \sum_{i=1}^k \lambda_i \cdot A_\sigma(\mathbf{x} - \boldsymbol{\mu}_i) \quad \text{for} \quad A_\sigma(\mathbf{z}) = \frac{1}{\pi\sigma^2} \left(\frac{J_1(\|\mathbf{z}\|_2/\sigma)}{\|\mathbf{z}\|_2/\sigma} \right)^2.$$

Note that the factor of $\frac{1}{\pi\sigma^2}$ in the definition of A_σ is to ensure that $A_\sigma(\cdot)$ is a probability density.

Also define

$$\Delta \triangleq \min_{i \neq j} \|\boldsymbol{\mu}_i - \boldsymbol{\mu}_j\|_2 \quad \text{and} \quad \mathcal{R} \triangleq \max_{i \in [k]} \|\boldsymbol{\mu}_i\|_2.$$

We now describe briefly how the parameters in Definition 2.1 translate to the setting of Fraunhofer diffraction by a circular aperture that we have outlined thus far. One should think of the spread parameter σ as $(\kappa r)^{-1}$. As σ in practice depends on known quantities pertaining to the underlying optical system, we assume henceforth that it is known *a priori*. The norm of the argument in $A_\sigma(\|\mathbf{x} - \boldsymbol{\mu}_i\|_2)$ corresponds to the quantity $\sin \theta$, where θ is the angle of displacement between the line from the center of the aperture to the center $\boldsymbol{\mu}_i$ of the i -th Airy disk, and the line between the center of the aperture and the point \mathbf{x} on the observation plane. Lastly, by Remark B.1, angular separation of ψ between two point sources translates to angular separation of ψ between the centers of their Airy disks on the observation plane. The parameters Δ and \mathcal{R} can thus be interpreted respectively as the minimum angular separation among the point sources, and the maximum angular distance of any of the point sources to the optical axis.

B.3 Comparison to Semiclassical Detection Model

In this section we clarify the distinctions between the model we study and the semiclassical detection model. We begin by formally defining the latter.

Definition B.1 (Semiclassical Detection Model). For $D = 1, 2$, let $S_1, \dots, S_m \subset \mathbb{R}^D$ be disjoint subsets corresponding to different regions of a photon detector, and suppose the detector receives some number N' of photons, where $N' \sim \text{Poi}(N)$. We observe photon counts N_1, \dots, N_m corresponding to the number of photons that interact with each region of the detector, where for each $i \in [m]$,

$$N_i \triangleq N'_i + \gamma_i, \quad N'_i \sim \text{Poi}(\lambda_i \cdot N), \gamma_i \sim \mathcal{N}(0, \sigma^2),$$

where $N'_1, \dots, N'_m, \gamma_1, \dots, \gamma_m$ are independent, γ_i represents white detector noise², and

$$\lambda_i \triangleq \int_{S_i} \rho(\mathbf{x}) \, d\mathbf{x},$$

where $\rho(\cdot)$, as in our model, is the idealized, normalized intensity profile of the optical signal.

²While these white noise terms $\{\gamma_i\}$ were not present in [Man59, Hel64], they are considered in some later treatments of this model, so we include them here for completeness.

To see how this relates to our model, first consider the idealized case where $\sigma = 0$ and that the different regions S_i of the detector form a partition of the entire ambient space. To get quantitative guarantees, existing works assume that each of these regions S_i is, e.g., a segment or box of fixed length ς . In this case, the semiclassical detection model is a special case of our model. Indeed, if one samples $\text{Poi}(N)$ points from ρ and moves each of them by distance $O(\varsigma)$ to the center of the region S_i of the photon detector to which they respectively belong, this collection of $O(\varsigma)$ -granular samples from ρ is identical in information and distribution to a sample of photon counts $\{N_i\}$ from the semiclassical detection model.

Our model can also capture the case where the regions S_i only partition a *subset* of the ambient space \mathbb{R}^D . In this case, we only get access to samples from the density $\rho_{\text{trunc}}(\mathbf{x}) \propto \mathbf{1}[\mathbf{x} \in \cup S_i] \cdot \rho(\mathbf{x})$, but this has known Fourier transform, given up to a universal multiplicative factor by the convolution of $\hat{\rho}$ with the indicator function of $\cup S_i$. So our techniques still apply in a straightforward fashion. In addition, by standard estimates on the tails of J_1 , for $\cup S_i$ of radius polynomially large in the relevant parameters, with high probability none of the samples used by our algorithms will fall outside of $\cup S_i$ to begin with. For these reasons, we will not belabor this point in this work and will assume $\cup S_i = \mathbb{R}^D$ throughout.

Lastly, while our model does not incorporate white detector noise σ , we note that our algorithms can nevertheless handle the semiclassical detection model with $\sigma > 0$: from a set of photon counts N_1, \dots, N_m , we can still estimate the Fourier transform of ρ to accuracy depending polynomially on N and inverse polynomially on σ and the sizes of the detector regions, so our techniques based on the matrix pencil method still apply.

B.4 A Menagerie of Diffraction Limits

In this section we give a precise characterization of the various limits that have appeared in the literature as candidates for the threshold at which resolution becomes impossible in diffraction-limited optical systems.

Abbe Limit The Abbe limit first arose in Abbe’s studies [Abb73] of the following setup in microscopy: light illuminates an idealized object, namely an diffraction grating consisting of infinitely many closely spaced slits corresponding to the fine features of the object being imaged, and passes through the slits, behind which is an aperture stop placed in the back focal plane of the lens. Abbe observed that the angle at which the light gets diffracted by the slits increases as the grating gets finer, and he calculated the point at which the angle is too wide to enter the aperture. This threshold is now called the *Abbe limit*, and in the modern language of Fourier optics, the Abbe limit corresponds to the point at which the Fourier transform of the corresponding point spread function (see Fact 1) vanishes. In the remainder of this section, we will refer to the Abbe limit as τ .

Remark B.2 (Scaling and Numerical Aperture). *The argument z in $A_\sigma(z)$ corresponds to the more familiar-looking quantity*

$$z = \frac{2\pi}{\lambda} \cdot a \sin \theta, \quad (23)$$

where λ is the average wavelength of illumination, a is the radius of the aperture, and θ is the angle of observation.

As noted above, $\widehat{A}_\sigma[\omega]$ is only supported on ω for which $\|\omega\| \leq \frac{1}{\pi}$. Equating this threshold $\frac{1}{\pi}$ with $1/z$, where z is given by (23), and rearranging, we conclude that $\sin \theta = \frac{\lambda}{2a}$. We may write $\sin \theta$ as q/R for q the distance between the observation point and the optical axis and R the distance between the observation point and the center of the aperture. It then follows that $q = \frac{\lambda R}{2a} \approx \frac{\lambda}{2NA}$, where NA is the numerical aperture. This recovers the usual formulation of the Abbe limit.

In the literature on super-resolution microscopy, the Abbe limit is the definition of diffraction limit that is usually given. Indeed, Lauterbach notes in his survey [Lau12] that “Abbe is perhaps the one who is most often cited for the notion that the resolution in microscopes would always be limited to half the wavelength of blue light.”

Rayleigh Criterion The Rayleigh criterion is the point at which the point spread function first vanishes. For $\sigma = 1$, this is precisely the smallest positive value of r for which $J_1(r) = 0$, which can be numerically computed to be $r \approx 3.83 \approx 1.22 \cdot \pi$. So for general σ , we conclude that the Rayleigh criterion is $\approx 1.22\tau$.

This is typically touted in standard references as the most common definition of resolution limit. Indeed, Weisenburger and Sandoghdar remark in their survey [WS15] that “Although Abbes resolution criterion is more rigorous, a more commonly known formulation...is the Rayleigh criterion.” Kenyon [Ken08] calls it the “standard definition of the limit of the resolving power of a lens system.” In his classic text, Hecht [Hec15] refers to it as the “ideal theoretical angular resolution” Rayleigh himself [Ray79] emphasized however that “This rule is convenient on account of its simplicity and it is sufficiently accurate in view of the necessary uncertainty as to what exactly is meant by resolution.” We refer to Appendix C for further quotations regarding the Rayleigh criterion.

Sparrow Criterion The Sparrow criterion, put forth in [Spa16], is the smallest Δ for which a superposition of two Δ -separated Airy disks becomes unimodal. Numerically, this threshold is $\approx 0.94\tau$.

The Sparrow limit is often cited as the most mathematically rigorous resolution criteria (in den Dekker and van de Bos’ survey [DDVdB97], they even call it “the natural resolution limit that is due to diffraction...even a hypothetical perfect measurement instrument would not be able to detect a central dip in the composite intensity distribution, simply because there is no such dip anymore.”). It is less relevant in practical settings as it requires perfect knowledge of the functional form of the point spread function. Again, we refer to Appendix C for further quotations regarding the Sparrow criterion.

Houston Criterion The Houston criterion is twice the radius at which the value of the density is half of its value at zero, i.e. the “full width at half maximum” (FWHM). This threshold is $\approx 1.03\tau$.

This measure is one of the most popular in practice where one does not have fine-grained knowledge of the point spread function, in particular because it can apply even when the point spread function in question does not fall exactly to zero, either due to noise or aberrations in the lens. In [DWS15] where the authors explore alternative means of assessing resolution in light of new super-resolution microscopy technologies, they remark in their conclusion that “the best approach to compare between techniques is still to perform the simple and robust fitting of a Gaussian to a sub-resolution object and then to extract the FWHM.”

Miscellaneous Additional Criteria The *Buxton limit* is nearly the same as Houtson, except it is the FWHM for the *amplitude* rather than the intensity, which yields a threshold of $\approx 1.46\tau$ [Bux37]. The *Schuster criterion* is defined to be twice the Rayleigh limit [Sch04], that is, two Airy disks are separated only when their central bands are disjoint, which yields a threshold of $\approx 2.44\tau$. The *Dawes limit*, which is $\approx 1.02\tau$, is a threshold proposed by Dawes [Daw67]; its definition is purely empirical, as it was derived by direct observation by Dawes.

C Debate Over the Diffraction Limit: A Historical Overview

In this section, we catalogue quotations from the literature relevant to the challenge of identifying the right resolution criterion, as well as to the need to take noise into account when formulating such definitions.

C.1 Identifying a Criterion

Since its introduction, the Rayleigh criterion has repeatedly been both touted as a practically helpful proxy by which to roughly assess the resolving power of diffraction-limited imaging systems, and characterized as somewhat arbitrary.

Rayleigh himself in his original 1879 work [Ray79]:

“This rule is convenient on account of its simplicity and it is sufficiently accurate in view of the necessary uncertainty as to what exactly is meant by resolution.”

Williams [Wil50, p. 79] in 1950:

“Although with the development of registering microphotomers such as the Moll, dips much smaller than [the one exhibited by a superposition of two Airy disks at the Rayleigh limit] can be accurately measured, it is convenient for the purpose of comparison with gratings and echelons to keep to this standard.”

Born and Wolf [BW13, p. 418] in 1960:

“The conventional theory of resolving power...is appropriate to direct visual observations. With other methods of detection (e.g. photometric) the presence of two objects of much smaller angular separation than indicated by Rayleighs criterion may often be revealed.”

Feynman [FLS11, Section 30-4] in his Lectures on Physics from 1964:

“...it seems a little pedantic to put such precision into the resolving power formula. This is because Rayleighs criterion is a rough idea in the first place. It tells you where it begins to get very hard to tell whether the image was made by one or by two stars. Actually, if sufficiently careful measurements of the exact intensity distribution over the diffracted image spot can be made, the fact that two sources make the spot can be proved even if θ is less than λ/L .”

Hecht in his standard text [Hec15, p.431,492] from 1987:

“We can certainly do a bit better than this, but Rayleigh’s criterion, however arbitrary, has the virtue of being particularly uncomplicated.”

“Lord Rayleigh’s criterion for resolving two equal-irradiance overlapping slit images is well-accepted, even if somewhat arbitrarily in the present application.”

In fact, as early as 1904, Schuster [Sch04, p. 158] made the same point and on the same page advocated for an alternative criterion, corresponding to twice the separation posited by Rayleigh:

“There is something arbitrary in (the Rayleigh criterion) as the dip in intensity necessary to indicate resolution is a physiological phenomenon, and there are other forms of spectroscopic investigation besides that of eye observation... It would therefore have been better not to have called a double line “resolved” until the two images stand so far apart, that no portion of the central band of one overlaps the central band of the other, as this is a condition which applies equally to all methods of observation. This would diminish to one half the at present recognized definition of resolving power.”

Ever since, the question of identifying the “right” notion of a resolution criterion has been periodically revisited in the literature.

Ramsay et al. [RCK41, p. 26] in 1941, on this problem’s theoretical and practical importance:

“Before the theory itself can be developed in full, and applied to the assignment of numerical values, it is necessary to consider the persistently vexing problem of criteria for a limit of resolution.”

Three decades after Ramsay’s work, Thompson [Tho69, p. 171]:

“The specification of the quality of an optical image is still a major problem in the field of image evaluation and assessment. This statement is true even when considering purely incoherent image formation.”

The Sparrow criterion is often regarded as the most mathematically rigorous resolution criterion.

Sparrow [Spa16, p. 80] in 1916 on its mathematical and physiological justification:

“It is obvious that the undulation condition should set an upper limit to the resolving power. The surprising fact is that this limit is apparently actually attained, and that the doublet still appears resolved, the effect of contrast so intensifying the edges that the eye supplies a minimum where none exists. The effect is observable both in positives and in negatives, as well as by direct vision...My own observations on this point have been checked by a number of my friends and colleagues.”

In the survey of den Dekker and van den Bos [DDVdB97, p. 548] eighty years later:

“Since Rayleigh’s days, technical progress has provided us with more and more refined sensors. Therefore, when visual inspection is replaced by intensity measurement, the natural resolution limit that is due to diffraction would be [the Sparrow limit]...even a hypothetical perfect measurement instrument would not be able to detect a central dip in the composite intensity distribution, simply because there is no such dip anymore.”

In light of advancements in super-resolution microscopy, rigorously characterizing the resolving power of imaging systems remains as pressing a challenge as ever.

In 2017, Demmerle et al. [DWSD15] revisited what resolution means in light of these new technologies and propose approaches for comparing resolution between different super-resolution methods. As they note in their introduction [DWSD15, p. 3]:

“The recent introduction of a range of commercial super-resolution instruments means that resolution has once again become a battleground between different microscope technologies and rival companies.”

Notably, in the conclusion, they remark that a classical Houston criterion-style approach is still the best for comparing different methods [DWSD15, p. 9].

“Given the above points, the best approach to compare between techniques is still to perform the simple and robust fitting of a Gaussian to a sub-resolution object and then to extract the FWHM.”

C.2 The Importance of Noise

An idea that has been repeated one way or another in the literature is that if one has perfect access to the *exact* intensity profile of the diffraction image of two point sources, then one could brute-force search over the space of possible parameters to find a hypothesis that fits the point spread function arbitrarily well, thereby learning the positions of the point sources regardless of their separation. As such, for any notion of diffraction limit to have practical meaning, it must take into account factors like aberrations and measurement noise that preclude getting perfect access to the intensity profile.

This perspective was distilled emphatically by di Francia [DF55, p. 497] in 1955:

“Moreover it is only too obvious that from the mathematical standpoint, the image of two points, however close to one another, is different from that of one point. It is not at all absurd to assume that technical progress may provide us with more and more refined kinds of receptors, detecting the difference between the image of a single point and the image of two points located closer and closer to another. This means that at present there is only a practical limit (if any) and not a theoretical limit for two-point resolving power.”

Contemporaneously, in discussions at the 1955 Meeting of the German Society of Applied Optics culminating in [Ron61, p. 459], Ronchi made the following distinction:

“Nowadays it seems imperative to differentiate three kinds of images, i.e., (1) the ethereal image, (2) the calculated image, and (3) the detected image.

The nature of the ethereal image should be physical, but in reality it is only a hypothesis. It is said that the radiant flux emitted by the object...is concentrated and distributed in the so-called image by means of a number of processes. But actually this is only a hypothesis...attempts have been made to give a mathematical representation of the phenomenon, both geometrically and algebraically...The images which have been calculated in this way...should therefore be called calculated images.

If we now consider the field of experience, we find the detected images. They are the figures either perceived by the eye when looking through the instrument, or obtained by means of a photosensitive emulsion, or through a photoelectric device.

den Dekker and van den Bos [DDVdB97, p. 547] in their 1997 survey:

“Since Ronchi’s paper, further research on resolution— concerning detected images instead of calculated ones— has shown that in the end, resolution is limited by systematic and random errors resulting in an inadequacy of the description fo the observations by the mathematical model chosen. This important conclusion was independently drawn by many researchers who were approaching the concept of resolution from different points of view.”

den Dekker and van den Bos summarize the state of affairs as follows [DDVdB97, p. 547]:

“If calculated images were to exist, the known two-component model could be fitted numerically to the observations with respect to the component locations and amplitudes. Then the solutions for these locations and amplitudes would be exact, a perfect fit would result, and in spite of diffraction there would be no limit to resolution no matter how closely located the two point sources; this would mean that no limit to resolution for calculated images would exist. However, imaging systems constructed without any aberration or irregularity are an ideal that is never reached in practice.... Therefore one should consider the resolution of detected images instead of calculated images.”

Goodman [Goo15, p. 326-7] in 2000:

“...the question of when two closely spaced point sources are barely resolved is a complex one and lends itself to a variety of rather subjective answers...An alternative definition is the so-called Sparrow criterion...In fact, the ability to resolve two point sources depends fundamentally on the signal-to-noise ratio associated with the detected image intensity pattern, and for this reason criteria that do not take account of noise are subjective.”

Maznev and Wright [MW17, p. 3] in 2016 on the earlier quote by Born and Wolf:

“Indeed, if any number of photons is available for the measurement, there is no fundamental limit to how well one can resolve two point sources, since it is possible to make use of curve fitting to arbitrary precision (however, there are obvious practical limitations related to the finite measurement time and other factors such as imperfections in the optical system, atmospheric turbulence, etc).”

Demmerle et al. in the work mentioned in the previous section [DWSD15, P. 9]:

“If one, a priori, knows that there are two point sources, then measuring their separation, and hence calculating the system’s resolution is purely limited by Signal-to-Noise Ratio.”

A related point that has been made repeatedly in the literature is that the original setting in which Abbe introduced his diffraction limit should not be conflated with the setting of resolving two point sources of light.

In the work of di Francia cited above [DF55, p. 498], he notes that the classic impossibility result for resolving a lattice of alternatively dark and bright points with separation below the Abbe limit says nothing about the impossibility of resolving a pair of points sources:

“[The impossibility result at the Abbe limit] has often been given a wrong interpretation and it has too hastily been extended to the case of two points. The [Abbe limit] applies only when we want the available information uniformly distributed over the whole image. Mathematics cannot set any lower limit for the distance of two resolvable points.”

Indeed, he argues informally, by way of the Nyquist sampling theorem, that when there is a prior on the number of components in a superposition of Airy disks being upper bounded by a known constant, then in theory, there is no diffraction limit. Rather, he posits, it is the entropy of the prior that dictates the limits of resolution [DF55, p. 498]:

“The fundamental question of how many independent data are contained in an image formed by a given optical instrument. This seems to be the modern substitute for the theory of resolving power.”

Sheppard [She17, p. 597] in 2017, sixty years after di Francia’s work, clarifies again that the abovementioned impossibility result should not be misinterpreted as saying anything about the impossibility of resolving two point sources:

“The Abbe resolution limit is a sharp limit to the imaging of a periodic object such as a grating. Super-resolution refers to overcoming this resolution limit. The Rayleigh resolution criterion refers to imaging of a two-point object. It is based on an arbitrary criterion, and does not define a sharp transition between structures being resolved or not resolved.”

D Proof of Lemma 3.7

TENSORRESOLVE (Algorithm 5) uses the standard subroutine given in Algorithm 7. We remark that this algorithm appears to be deterministic unlike usual treatments of Jennrich’s algorithm simply because we have absorbed the usual randomness of the choice of flattening into the construction of the tensor \mathbf{T} on which TENSORRESOLVE calls JENNRICH.

Algorithm 7 JENNRICH($\tilde{\mathbf{T}}$)

- 1: **Input:** Tensor $\tilde{\mathbf{T}} \in \mathbb{C}^{m \times m \times 3}$ which is close to a rank- k tensor \mathbf{T} of the form (7)
 - 2: **Output:** $\hat{V} \in \mathbb{C}^{m \times k}$ close to V up to column permutation (see Lemma 3.7)
 - 3: Compute the k -SVD $\hat{P}\hat{\Lambda}\hat{P}^\dagger$ of the flattening $\tilde{\mathbf{T}}(\text{Id}, \text{Id}, e_1)$.
 - 4: Define the whitened tensor $\hat{\mathbf{E}} = \tilde{\mathbf{T}}(\hat{P}, \hat{P}, \text{Id})$ and its flattenings $\hat{E}_i \triangleq \hat{\mathbf{E}}(\text{Id}, \text{Id}, e_i)$ for $i \in [2]$.
 - 5: Define $\hat{M} \triangleq \hat{E}_1 \hat{E}_2^{-1}$.
 - 6: Form the matrix \hat{U} whose columns are equal to the eigenvectors, scaled to have norm \sqrt{m} , for the k eigenvalues of \hat{M} that are largest in absolute value.
 - 7: Output $\hat{V} \triangleq \hat{P}\hat{U}$.
-

We restate Lemma 3.7 here for the reader’s convenience:

Lemma 3.7. [e.g. [HK15], Lemma 3.5] For any $\epsilon, \delta > 0$, suppose $|\mathbf{T}_{a,b,i} - \tilde{\mathbf{T}}_{a,b,i}| \leq \eta'$ for $\eta' \triangleq O\left(\frac{(c-\gamma_{\text{res}})\delta\Delta\lambda_{\min}^2}{k^5/2m^3/2\kappa(V)^5} \cdot \epsilon\right)$, and let $\hat{V} = \text{JENNRICH}(\tilde{\mathbf{T}})$ (Algorithm 7). Then with probability at least $1 - \delta$ over the randomness of $v^{(1)}$, there exists permutation matrix Π such that $\|\hat{V} - V\Pi\|_F \leq \epsilon$ for all $j \in [k]$.

This proof closely follows that of [HBZ10], though we must make some modifications because the scaling of the frequencies $v^{(i)}$ for $i \in [3]$ defined in Step 5 of TENSORRESOLVE is different.

Proof. We first define the noiseless versions of the objects $\hat{P}, \hat{\Lambda}, \hat{E}, \hat{E}_1, \hat{E}_2, \hat{M}, \hat{U}$ introduced in JENNRICH. Note that for $i \in [2]$,

$$\mathbf{T}(\text{Id}, \text{Id}, e_i) = V D_i V^\dagger \tag{24}$$

for D_i the diagonal matrix whose diagonal entries are given by $\{\lambda_j e^{-2\pi i \langle \mu_j, v^{(i)} \rangle}\}_{j \in [k]}$. Denote the k -SVD of $\mathbf{T}(\text{Id}, \text{Id}, e_1)$ by $P\Lambda P^\dagger$. Define the whitened tensor $\mathbf{E} \triangleq \mathbf{T}(P, P, \text{Id})$ and its flattenings

$E_i = \mathbf{E}(\text{Id}, \text{Id}, e_i)$ for $i \in [2]$. Finally, define $U \triangleq P^\dagger V$ so that

$$\mathbf{E} = \sum_{j=1}^k \lambda_j U^j \otimes U^j \otimes W^j$$

and $E_i = U D_i U^\dagger$ for $i \in [2]$. Note that U also satisfies $M \triangleq E_1 E_2^{-1} = U D U^\dagger$ for diagonal matrix $D \triangleq D_1 D_2^{-1}$, and for every $j \in [k]$, $\|U^j\|_2 = \|V^j\|_2 = \sqrt{m}$, so U is indeed the noiseless analogue of \hat{U} .

For any $j \in [k]$, we have that

$$D_{j,j} = e^{-2\pi i \langle \mu_j, v^{(1)} - v^{(2)} \rangle}.$$

Define $\Delta_D \triangleq \min_{j \neq j'} |D_{j,j} - D_{j',j'}|$.

For every $j, j' \in [k]$, by triangle inequality and the fact that $V^j = P U^j$ and $\hat{V} = \hat{P} \hat{U}^j$, we have

$$\|\hat{V}^j - V^{j'}\|_2 \leq \|\hat{P} - P\|_2 \|\hat{U}^j\|_2 + \|P\|_2 \|\hat{U}^j - U^{j'}\|_2 \leq \sqrt{m} \|\hat{P} - P\|_2 + \|\hat{U}^j - U^{j'}\|_2. \quad (25)$$

We proceed to upper bound $\|\hat{P} - P\|_2$ and $\|\hat{U}^j - U^{j'}\|_2$.

Lemma D.1. $\|\hat{P} - P\|_2 \leq \frac{\eta' \sqrt{m}}{\lambda_{\min} \sigma_{\min}(V)^2}$.

Proof. By Wedin's theorem,

$$\|\hat{P} - P\|_2 \leq \frac{\|\tilde{\mathbf{T}}(\text{Id}, \text{Id}, e_1) - \mathbf{T}(\text{Id}, \text{Id}, e_1)\|_2}{\sigma_{\min}(\mathbf{T}(\text{Id}, \text{Id}, e_1))}.$$

By (24), $\sigma_{\min}(\mathbf{T}(\text{Id}, \text{Id}, e_1)) \geq \lambda_{\min} \sigma_{\min}(V)^2$. Additionally, $\|\tilde{\mathbf{T}}(\text{Id}, \text{Id}, e_1) - \mathbf{T}(\text{Id}, \text{Id}, e_1)\|_F \leq \eta' \sqrt{m}$, from which the claim follows. \square

Lemma D.2. *If $\|M - \hat{M}\|_2 \leq \frac{\Delta_D}{2\sqrt{k\kappa}(U)}$, then the eigenvalues of \hat{M} are distinct, and there exists a permutation τ for which*

$$\|\hat{U}^j - U^{\tau(j)}\|_2 \leq \frac{3m \|M - \hat{M}\|_2}{\Delta_D \sigma_{\min}(U)} \quad \forall j \in [k].$$

Proof. Consider the matrix $U^{-1} \hat{M} U = D - U^{-1} (M - \hat{M}) U$. Because $\|U^{-1} (M - \hat{M}) U\|_2 \leq \Delta_D / 2\sqrt{k}$ by assumption, we conclude by Gershgorin's that the eigenvalues of $U^{-1} \hat{M} U$, and thus of \hat{M} , are distinct and each lies within $\Delta_D / 2$ of a unique eigenvalue of M . Let τ be the permutation matching eigenvalues $\{\hat{\beta}_j\}$ of \hat{M} to eigenvalues $\{\beta_j\}$ of M which are closest, and without loss of generality let τ be the identity permutation.

For fixed $j \in [k]$, let $\{c_{j'}\}$ be coefficients for which $\hat{U}^j = \sum c_{j'} U^{j'}$ and $\sum_{j'} c_{j'}^2 = 1$. Note that we have

$$\hat{\lambda}_j \sum_{j'} c_{j'} U^{j'} = \hat{\lambda}_j \hat{U}^j = \hat{M} \hat{U}^j = \sum_{j'} \lambda_{j'} c_{j'} U^{j'} + (M - \hat{M}) \hat{U}^j,$$

so $\{c_{j'}\}$ is the solution to the linear system

$$\sum_{j'} c_{j'} \cdot (\hat{\lambda}_j - \lambda_{j'}) U^{j'} = (M - \hat{M}) \hat{U}^j.$$

Recalling that $\|U^j\|_2 = \sqrt{m}$ and that $\sum c_{j'}^2 = 1$, we get that

$$\begin{aligned} \|\hat{U}^j - U^j\|_2^2 &= \sum_{j' \neq j} c_{j'}^2 \|U^{j'}\|_2^2 + (c_j - 1)^2 \|U^j\|_2^2 \leq 2m \sum_{j' \neq j} c_{j'}^2 \\ &\leq \frac{8m \|U^{-1}(M - \hat{M})\hat{U}^j\|_2^2}{\Delta_D^2} \leq \frac{8m^2 \|M - \hat{M}\|_2^2}{\Delta_D^2 \sigma_{\min}(U)^2}. \end{aligned}$$

□

Finally, we must estimate $\|M - \hat{M}\|_2^2$ in the bound in Lemma D.2:

Lemma D.3. *If $\eta' \leq \frac{\lambda_{\min}^2 \sigma_{\min}(V)^2}{6\sqrt{m}\kappa(V)^2}$, then $\|M - \hat{M}\|_2 \leq \frac{9\eta' \sqrt{m}\kappa(V)^2}{\lambda_{\min}^2 \sigma_{\min}(V)^2}$.*

Proof. Define $Z_i \triangleq \hat{E}_i - E_i$ for $i \in [2]$ so by taking Schur complements

$$M - \hat{M} = E_1 E_2^{-1} - (E_1 + Z_1)(E_2 + Z_2)^{-1} = M Z_2 (\text{Id} + E_2^{-1} Z_2)^{-1} E_2^{-1} + Z_1 E_2^{-1} \triangleq MH + G \quad (26)$$

Note that

$$\sigma_{\max}(H) \leq \frac{\|Z_2\|_2}{\sigma_{\min}(E_2) - \|Z_2\|_2} \leq \frac{\|Z_2\|_2}{\lambda_{\min} \sigma_{\min}(U)^2 - \|Z_2\|_2}, \quad \sigma_{\max}(G) \leq \frac{\sigma_{\max}(Z_1)}{\sigma_{\min}(E_2)} \leq \frac{\|Z_1\|_2}{\lambda_{\min} \sigma_{\min}(U)^2}$$

and furthermore for either $i \in [2]$, because $Z_i = \hat{P}^\dagger \tilde{\mathbf{T}}(\text{Id}, \text{Id}, e_i) \hat{P} - P^\dagger \mathbf{T}(\text{Id}, \text{Id}, e_i) P$,

$$\begin{aligned} \|Z_i\|_2 &\leq \|P\|_2 \|\mathbf{T}(\text{Id}, \text{Id}, e_i)\|_2 \|P - \hat{P}\|_2 + \|\hat{P}\|_2 \|\mathbf{T}(\text{Id}, \text{Id}, e_i)\|_2 \|\hat{P} - P\|_2 + \|\hat{P}\|_2^2 \|\tilde{\mathbf{T}}(\text{Id}, \text{Id}, e_i)\|_2 \\ &\leq 2 \frac{\eta' \sqrt{m}}{\lambda_{\min} \sigma_{\min}(V)^2} \cdot \lambda_{\max} \sigma_{\max}(V)^2 + \lambda_{\max} \sigma_{\max}(V)^2 \leq \frac{3\eta' \sqrt{m}\kappa(V)^2}{\lambda_{\min}} \end{aligned} \quad (27)$$

Because $\sigma_{\min}(U)^2 = \sigma_{\min}(V)^2$, by the bound on η' in the hypothesis, $\sigma_{\max}(H) \leq \frac{2\|Z_2\|_2}{\lambda_{\min} \sigma_{\min}(V)^2}$. Finally, noting that $\|M\|_2 \leq \sigma_{\max}(D) = 1$, we conclude the proof from (26) and (27). □

It remains to bound Δ_D .

Lemma D.4. *For any $\delta > 0$, with probability at least $1 - \delta$, $\Delta_D \geq O\left(\frac{(c - \gamma_{\text{res}})\delta' \Delta}{k^2}\right)$.*

Proof. Using the elementary inequality $|e^{-2\pi i x} - 1| \leq 2\pi|x|$ for any $x \in \mathbb{R}$, we conclude that $|D_{j,j} - D_{j',j'}| \leq |e^{-2\pi i \langle \mu_j - \mu_{j'}, v^{(1)} - v^{(2)} \rangle} - 1| \leq 2\pi |\langle \mu_j - \mu_{j'}, v^{(1)} - v^{(2)} \rangle|$. By standard anti-concentration, for any $j \neq j'$ and $\delta' > 0$ we have that $|\langle \mu_j - \mu_{j'}, v^{(1)} - v^{(2)} \rangle| \leq O(\delta' \|\mu_j - \mu_{j'}\|_2 \cdot \|v^{(1)} - v^{(2)}\|_2)$ with probability at most δ' . The proof follows by taking $\delta' = \delta/k^2$, union bounding, and recalling the definition of $v^{(1)}, v^{(2)}$ in TENSORRESOLVE. □

Combining (25) and Lemmas D.1, D.2, D.3, D.4, there exists a permutation τ for which

$$\|\hat{V}^j - V^{\tau(j)}\|_2 \leq \frac{\eta' m}{\lambda_{\min} \sigma_{\min}(V)^2} + \frac{27\eta' m^{3/2} \kappa(V)^2}{\Delta_D \lambda_{\min}^2 \sigma_{\min}(V)^3} \leq O\left(\frac{k^2 \eta' m^{3/2} \kappa(V)^5}{(c - \gamma_{\text{res}}) \delta \Delta \lambda_{\min}^2}\right) \quad \forall j \in [k].$$

We conclude that for the permutation matrix Π corresponding to τ , $\|\hat{V} - V\Pi\|_F \leq \sqrt{k} \max_{j \in [k]} \|\hat{V}^j - V^{\tau(j)}\|_2 \leq O\left(\frac{k^{5/2} \eta' m^{3/2} \kappa(V)^5}{(c - \gamma_{\text{res}}) \delta \Delta \lambda_{\min}^2}\right)$ as claimed. □

E Generating Figure 3

Here we elaborate on how Figure 3 was generated. While Theorem 4.1 yields an explicit construction which rigorously demonstrates the phase transition at the diffraction limit, empirically we found that this phase transition was even more pronounced when we slightly modified the construction. Specifically, we empirically evaluated the following instance: for even k , separation $\Delta > 0$, and $1 \leq i \leq k$, let $\boldsymbol{\mu}_i = (a_i, 0)$ and let $\boldsymbol{\mu}'_i = (b_i, 0)$ for $a_i \triangleq \frac{\Delta}{2} \cdot (2i - \frac{k+3}{2})$ and $b_i \triangleq \frac{\Delta}{2} \cdot (2i - \frac{k+1}{2})$, and take $\{\lambda_i\}$ and $\{\lambda'_i\}$ to be the unique solution to the affine system

$$\sum_{i=1}^{\lfloor k/2 \rfloor} \lambda_i = 1 \text{ and } \sum_{i=1}^{\lfloor k/2 \rfloor} \lambda'_i = 1 \quad \sum_{i=1}^{\lfloor k/2 \rfloor} \lambda_i a_i^\ell = \sum_{i=1}^{\lfloor k/2 \rfloor} \lambda'_i b_i^\ell \quad \forall 0 \leq \ell < k - 1.$$

These are the weights for which the superposition of point masses at $\{\boldsymbol{\mu}_i\}$ with weights $\{\lambda_i\}$ matches the superposition of point masses at $\{\boldsymbol{\mu}'_i\}$ with weights $\{\lambda'_i\}$ on all moments of degree at most $k - 2$. While moment-matching does not directly translate to any kind of statistical lower bound, it is often the starting point for many such lower bounds in the distribution learning literature [MV10, DKS17, HP15, Kea98]. The “carefully chosen pair of superpositions” referenced in the caption of Figure 3 refers to this moment-matching construction. Henceforth refer to these two superpositions, both of which are Δ -separated superpositions of $k/2$ Airy disks, as $\mathcal{D}_0(\Delta, k)$ and $\mathcal{D}_1(\Delta, k)$ respectively. We will omit the parenthetical Δ, k when the context is clear.

Unfortunately, there is no closed form for the expression for $d_{\text{TV}}(\mathcal{D}_0, \mathcal{D}_1)$. Instead, we estimated this via numerical integration. Direct evaluation of the integral $\int_{\mathbb{R}^2} |\mathcal{D}_0(\mathbf{x}) - \mathcal{D}_1(\mathbf{x})| d\mathbf{x}$ poses issues because of the heavy tails of the Airy point spread function. To tame these tails, we used a carefully chosen proposal measure μ in order to rewrite $d_{\text{TV}}(\mathcal{D}_0, \mathcal{D}_1)$ as $\int_{\mathbb{R}^2} \left| \frac{\mathcal{D}_0(\mathbf{x})}{\mu(\mathbf{x})} - \frac{\mathcal{D}_1(\mathbf{x})}{\mu(\mathbf{x})} \right| d\mu$. Because of the heavy tails, we needed to use a similarly heavy-tailed proposal distribution, so we took μ to be the convolution of the superposition of point masses at $\{\boldsymbol{\mu}_i\} \cup \{\boldsymbol{\mu}'_i\}$ having weights $\{\lambda_i\} \cup \{\lambda'_i\}$ with the following kernel $P(\cdot)$. To sample from the density over \mathbb{R}^2 corresponding to P , with probability $1/2$ sample a radius r uniformly from $[0, 1]$ and output a random vector in \mathbb{R}^2 of norm r , and with the remaining probability $1/2$, sample from the Pareto distribution with parameter $2/3$ over $[1, \infty]$ and output a random vector of norm r . The motivation for P and in particular for the parameter $2/3$ is that it is a rough approximation to the tail behavior of the radial density $\frac{J_1(r)^2}{r}$ defining the Airy point spread function, which by Theorem 2.1 decays roughly as $r^{-5/3}$.

To generate the curves in Figure 3, for each $k \in [2, 4, 6, 12, 20, 30, 42, 56, 72, 90]$ and each $\Delta \in [-2, -1.92, -1.84, \dots, 1.84, 1.92, 2]$, we simply estimated the corresponding $d_{\text{TV}}(\mathcal{D}_0, \mathcal{D}_1)$ by sampling 10 million points \mathbf{x} from μ and computing the empirical mean of the quantity $\left| \frac{\mathcal{D}_0(\mathbf{x})}{\mu(\mathbf{x})} - \frac{\mathcal{D}_1(\mathbf{x})}{\mu(\mathbf{x})} \right|$.

We have made the code for Figure 3 available at <https://github.com/secanth/airy/>.